Stony Brook University

Theoretical Considerations for Coherent Electron Cooling

A Dissertation Presented

by

Stephen Webb

to

The Graduate School

in Partial Fulfillment of the Requirements

for the Degree of

Doctor of Philosophy

in

Physics

Stony Brook University

May 2011

Stony Brook University

The Graduate School

Stephen Webb

We, the dissertation committee for the above candidate for the Doctor of Philosophy degree, hereby recommend acceptance of this dissertation.

Vladimir Litvinenko – Dissertation Advisor
Professor, Department of Physics and Astronomy

Thomas Hemmick – Chairperson of Defense
Distinguished Teaching Professor, Department of Physics and Astronomy

Paul Grannis
Distinguished Professor Emeritus, Department of Physics and Astronomy

Maria Fernandez-Serra
Assistant Professor, Department of Physics and Astronomy

Vadim Ptitsyn
Staff Scientist
Collider-Accelerator Department, Brookhaven National Laboratory

This dissertation is accepted by the Graduate School.

Lawrence Martin
Lawrence Martin
Dean of the Graduate School

Abstract of the Dissertation

Theoretical Considerations for Coherent Electron Cooling

by

Stephen Webb

Doctor of Philosophy

in

Physics

Stony Brook University

2011

Coherent electron cooling (CeC) offers the potential a very potent method of longitudinal phase-space cooling for high intensity bunched beam accelerators, such as at the Relativistic Heavy Ion Collider (RHIC) or at proposed electron-ion colliders such as eRHIC or LHeC. To develop a complete theoretical description of CeC requires a detailed model of the phase space dynamics of a high-gain free-electron laser (FEL) in three dimensions. A three-dimensional model for the FEL instability is developed using the Maxwell-Vlasov formalism, and obtains a Green function for arbitrary initial phase space perturbations. This Green function assumes a transversely infinite electron beam with zero transverse

velocity spread. The formalism developed for obtaining the Green function also provides a solution to the initial value problem of an FEL with a finite transverse beam, and this formalism is used to obtain optical guiding.

Using the resulting dispersion relation for the FEL process, I present a number of theorems and results concerning the roots of the dispersion relation, in particular that regardless of the specific functional form of the thermal background of the beam there is one and only one amplifying mode. A number of criterion and relations on that mode is also developed and presented.

Finally, I develop a theoretical description of the dynamics of Coherent Electron Cooling considering the case of a finite length electron bunch which paints the longer hadron bunch. This leads to a kinetic equation for the cooling of synchrotron oscillations in bunched beams.

To those that I love.

Contents

Bibliography   109

List of Figures

List of Tables

Acknowledgements

It takes a village to raise a graduate student, and for all their work, someone may get only a brief mention in the acknowledgements. But because of that fleeting moment of recognition, it is doubly important to include everyone who helped get through the ordeal of graduate school.

I would first like to thank my advisor, Vladimir Litvinenko, for providing the interesting problem of Coherent Electron Cooling, and keeping me on the right track even when I would wander a bit. I would also like to thank Gang Wang for the fruitful conversations and collaborative efforts in developing the research that make up this dissertation. Other members of C-AD at Brookhaven who proved helpful in conversations on physics as well as life include Todd Satogata, whose endless good-natured disposition always made a rough time feel better; Mike Blaskiewicz, for providing endless interesting ideas for problems I would encounter, even if he mainly served as a wall to bounce ideas off; Jörg Kewisch, for always taking an interest in my work and requiring me to keep my ideas straight; and finally the support staff, Annabelle Petway, Marion Heimerle, Gladys Blas, Pamela Manning, and anyone else who

1

Introduction

Free electron laser (FEL) based Coherent Electron Cooling (CeC) requires a detailed understanding of the phase space density of the FEL instability, as well as a firm understanding of the cooling kinetics. In this dissertation, I present work on both projects, broken into two parts.

In the first part of the dissertation I discuss developments in the theory of small-signal high-gain free electron lasers, particularly results on the propagation of an initial phase space perturbation through the FEL process. In

this part, I begin by introducing the basic theory of one-dimensional low-gain FELs to develop insight into the physics behind the FEL process. I then present a derivation of a Green function for an infinitely large, transversely cold electron bunch in an FEL undulator, and results obtained for a finite width, transversely cold bunch. In the final section I discuss analytical results concerning the nature of the dispersion relation for the FEL instability.

The second part is a study of the cooling kinetics of CeC, in particular a single-particle study of the equations of motion when considering the slowly varying electron bunch density and this effect on the cooling equations for CeC. In this section I present analytical as well as numerical results to understand the kinetics of CeC in greater detail.

The appendix of this dissertation is exhaustive, and is intended to be used as a reference for topics that may not be familiar to the reader. Many of the mathematical techniques used in the research leading to this dissertation are not standard fare a physicist is likely to encounter in a standard Ph.D. course. As such a variety of topics from least-action integrals to explanations of the choice of gauge are discussed, as well as an exhaustive review of relevant subjects from complex analysis and the theory of Laplace transforms.

1.1   Three-dimensional FEL Theory

In the first part, I detail a derivation for a three-dimensional model of the FEL amplification process using a coupled Maxwell-Vlasov approach to linearized perturbation theory. This leads to a closed form expression in Fourier space for the amplification process in terms of the thermal distribution of the

electron bunch. From this the FEL dispersion relation is derived for both finite and infinite transverse bunches.

Evaluation of the dispersion relation that results from this treatment is the subject of the following chapter. In standard perturbation theory, a gaussian energy distribution is analytically intractable, and so an approximation using $\kappa - N$ distribution functions is used. This approximation has the side effect that it predicts there to be $N + 2$ modes to the initial value problem. I then prove that, for an arbitrary single-peak energy distribution, there is at most one amplifying mode, and derive an analytical expression for the critical frequency above which the mode stops amplifying frequencies. This result is independent of the particular functional form of the energy distribution, and may be regarded as a topological quantity of the FEL dispersion relation.

1.2   CeC Kinetics

The second part of this dissertation is dedicated to developing the kinetic theory of Coherent Electron Cooling from a first principles calculation. I consider the case of electron bunches that are short compared to the hadron bunches they cool. This leads to two new effects to consider in the theoretical description of CeC [1]: a locally variable gain length in the FEL and a painting scheme.

The local variability of the gain length leads to an RF phase dependent phase slip in the cooling rate, as well as a suppressed cooling rate due to the lower gain in regions of lower density. The painting scheme is used to compensate for having the electron bunches shorter than the hadron bunches,

and involves sweeping the hadron bunches with electron bunches over many turns. In practice there are many synchrotron oscillations in a single painting sweep, and many painting sweeps over the cooling time, and this hierarchy of time scales allows a number of averaging approximations.

By carrying out this averaging, I develop an equation for the evolution of the envelope function as a function of the painting scheme. From this equation, it is possible to write down a kinetic equation which includes intra-beam scattering, synchrotron oscillations, and the cooling rate for Coherent Electron Cooling.

Part I

Free-Electron Laser Theory

2

Background – Free Electron Lasers

Free electron lasers are devices in which an electron bunch is made to coherently synchrotron radiate, thereby producing an almost monochromatic light pulse. A description of the configuration of FELs was first written down by John Madey [2] and later first demonstrated by Madey in 1977 [3]. The equations for high-gain FELs were first written down by Kondratenko and Saldin [4], with a simplified picture developed by Bonifacio, Narducci and Pellegrini [5] and a phase-space evolution picture using the Maxwell-Vlasov

formalism presented by Saldin, Schneidmiller and Yurkov [6].

In this section, I present the theory of FELs with a single-particle phase space picture, which contrasts with the treatment using the Maxwell-Vlasov equations in later chapters. While the mathematical formalism of the Maxwell-Vlasov equation is more germane to later work, I believe that the phase space picture is more intuitive and therefore more useful for understanding the physics behind the Maxwell-Vlasov treatment to be presented. I first present a description of the physical set-up of an FEL, with a schematic overview of undulator radiation. Then I develop the equations of motion which lead to the effective hamiltonian and ponderomotive potential and phase. Finally, I calculate an expression for the gain of a low-gain FEL, and describe how the high-gain regime is reached.

2.1 Undulator Radiation

An undulator is a configuration of alternating polarity magnetic fields running along a beam pipe. Its magnetic flux density may be modelled as

$$\boldsymbol{B}_u = B_0 \cos(k_u z) \; \hat{e}_x - B_0 \sin(k_u z) \; \hat{e}_y \qquad (2.1)$$

where $k_u = 2\pi/\lambda_u$ is the undulator wave number. For this and all future work, we assume an helical undulator. For an electron with energy $\gamma m c^2$, the electron will undergo transverse oscillations approximately given by

$$\boldsymbol{v}_\perp \approx -\frac{e\beta_z}{\gamma m c}\hat{e}_z \times \boldsymbol{B}_u \qquad (2.2)$$

where β_z is the relativistic $\boldsymbol{\beta}$, and for almost all applications is approximately unity. For the purposes of FEL applications, $\beta_z \approx 1$ with some small corrections that scale as γ^{-2}. Roughly speaking, the angle of deflection in this sinusoidal velocity is given by

$$\tan\theta = v_\perp/v_z \approx \frac{eB_u}{k_u \gamma m c^2} \tag{2.3}$$

Through physical arguments, one can also obtain the resonant frequency before actually obtaining the equations of motion. By analysing the velocity equation, the electrons in the bunch will clearly oscillate transversely with a phase $k_u z$. When this is in phase with the radiation field, which oscillates with phase $\omega_r(z/c - t)$, resonance will occur.

Defining the *ponderomotive phase* $\psi = k_u z + \omega_r(z/c - t)$, the resonance will occur when

$$\frac{d\psi}{dz} = k_u + \omega_r/c - \omega_r \frac{dt}{dz} = 0 \tag{2.4}$$

By observing that $\gamma^{-2} = 1 - \boldsymbol{\beta}_\perp^2 - \beta_z^2$, that $dt/dz = 1/(c\beta_z)$, and that $\boldsymbol{\beta}_\perp^2 = K^2/\gamma^2$ for an helical undulator, this obtains the resonance condition

$$\omega_r/c = -k_u \times \left(1 - \frac{1}{\sqrt{1 - (1/\gamma^2 + K^2/\gamma^2)}}\right)^{-1} \approx \frac{k_u}{2\gamma^2}(1 + K^2) \tag{2.5}$$

This is the exact resonance frequency for an undulator, and will be rigorously derived later. It is convenient for now to explain heuristically the origins of the resonance frequency. It is also worth noting here that a similar resonance condition occurs for planar undulators, but since $\beta_\perp^2 \propto \sin^2(k_u z)$ there are higher harmonics above the resonance generated, and in general much more

complicated behaviour. I therefore limit my discussion to helical undulators, which are more convenient to describe from a theoretical standpoint.

2.2   Single Particle Equations of Motion

For this section, I provide a derivation of the single particle equations of motion, following along derivations present in [7], [8] and others. I consider here a *seeded FEL*, one in which an initial laser field drives the FEL instability to produce further gain. For a seeding laser field at frequency ω, the FEL will produce coherent radiation at the frequency ω, but the gain will suffer if $\omega - \omega_r$ is too large. What constitutes "too large" will become apparent in this derivation.

From the relativistic energy equation, the energy transfer between the electron and a seeding laser field is given by

$$\frac{d\mathcal{E}}{dt} = -e\boldsymbol{v}_\perp \cdot \boldsymbol{E}_\perp \tag{2.6}$$

where $\boldsymbol{E}_\perp = E_0\left(\hat{e}_x \cos[\omega(z/c - t)] + \hat{e}_y \sin[\omega(z/c - t)]\right)$ is the helically polarized laser field at frequency ω. From this, it is clear that

$$\frac{d\mathcal{E}}{dz} = -\frac{e}{v_z}(v_x E_x + v_y E_y) \tag{2.7}$$

After some manipulation this leads to the equation for energy transfer

$$\frac{d\mathcal{E}}{dz} = -e\frac{K}{\gamma}\cos\psi \tag{2.8}$$

Here it should be clear that maximum gain would occur of ψ remained a constant, which is the origin of the resonance condition. It is furthermore worth noting that we have assumed that $\boldsymbol{E}_\perp$ is not changing appreciably with time, *i.e.* the beam does not appreciably change $\boldsymbol{E}_\perp$ enough to change the dynamics of the individual particles. This is the fundamental property of the low-gain limit, and when the modified laser field is self-consistently included in the equations of motion, the high-gain regime can be obtained.

Finally, we must include the dynamics of the ponderomotive phase, which are given by

$$\frac{d\psi}{dz} = k_u + \frac{\omega}{c} - \frac{\omega}{v_z} \tag{2.9}$$

Noting that $v_z \approx c$ and $dv_z/d\mathcal{E}\,|_{\mathcal{E}=\mathcal{E}_0} \approx c(1+K^2)/(\gamma^2\mathcal{E}_0)$, then for a bunch with sufficiently small energy spread it is sufficient to write

$$\frac{d\psi}{dz} = k_u + \frac{\omega}{c} - \frac{\omega}{c} + \frac{\omega}{c^2}\frac{c(1+K^2)}{\gamma^2\mathcal{E}_0}(\mathcal{E}-\mathcal{E}_0) \tag{2.10}$$

Consolidating the notation here by writing that

$$P = \mathcal{E} - \mathcal{E}_0$$

$$C = k_u + \frac{\omega}{c} - \frac{\omega}{v_z(\mathcal{E}_0)} = (\omega - \omega_r)/c$$

yields the effective equations of motion

$$\frac{dP}{dz} = -e\frac{K}{\gamma}\cos\psi \tag{2.11a}$$

$$\frac{d\psi}{dz} = C + \frac{\omega(1 + K^2)}{c\gamma^2 \mathcal{E}_0} P \qquad (2.11\text{b})$$

These appear to come from some effective hamiltonian with P and ψ as canonically conjugate variables. The effective hamiltonian is then given by

$$\mathcal{H} = CP + \frac{\omega(1 + K^2)}{2c\gamma^2 \mathcal{E}_0} P^2 + e\frac{K}{\gamma}\sin\psi \qquad (2.12)$$

Because this hamiltonian is independent of z, the (P, ψ) trajectories in phase space will move along lines of constant $\mathcal{H}$, but this effective hamiltonian is clearly not the energy since the energy $\mathcal{E}$ is not conserved.

2.3 Power Balance and Gain Calculation

It is fruitful to consider how much gain is actually made in this scheme. Gain can be calculated by conservation of energy arguments, in which the power lost from the electron bunch goes entirely into the radiation field. Calculating the full laser field is a difficult task, but obtaining the total energy loss of the beam as a function of z is an exercise in perturbation theory that yields directly an expression for the total power gain for the seeded laser field.

To begin the perturbation calculation, consider the case where the beam is monoenergetic[1], so that $P = 0$ for all particles in the bunch. The canonical expansion is to consider order by order beginning with $P^{(0)} = 0$. Then, to zeroth order

$$\psi^{(0)}(z) = Cz + \psi_0 \qquad (2.13)$$

---

[1]Accounting for a beam with finite energy spread is relatively simple and can be taken into account when averaging occurs. For brevity, I omit this effect, as it will be studied in greater detail in Chapter 3.

Iterating to first order gives an expression for $P^{(1)}(z)$. Inserting $\psi^{(0)}$ into the equation of motion for the energy at first order gives

$$P^{(1)} = -e\frac{K}{\gamma}E\int_0^z dz\ \cos(\psi^{(0)}(z)) = -e\frac{K}{\gamma}E\left(\sin(Cz+\psi_0) - \sin(\psi_0)\right) \quad (2.14)$$

Inserting this expression back to the equation for $\psi^{(1)}$, gives that

$$\begin{aligned}
\psi^{(1)} &= \frac{\omega(1+K^2)}{c\gamma^2\mathcal{E}_0}\int_0^z dz\ P^{(1)}(z) \\
&= \frac{\omega(1+K^2)}{c\gamma^2\mathcal{E}_0}\frac{eK}{\gamma}E\left[\frac{\cos(Cz+\psi_0)-\cos(\psi_0)}{C} - \sin(\psi_0)z\right] \quad (2.15)
\end{aligned}$$

The average of P vanishes to first order, so to obtain the power lost from the electron bunch requires taking P to second order. Inserting the first order for ψ back into the equations gives

$$P^{(2)} = -eKE/\gamma\int dz\ \cos(\psi_0 + Cz + \psi^{(1)}(z)) \quad (2.16)$$

By averaging P, over ψ_0, which for a bunched beam is done by integrating over the measure $(2\pi)^{-1}\int_0^{2\pi} d\psi_0$, the power generated by the beam in a single pass is given by

$$\Pi = -\frac{j_0\langle P\rangle}{e} \quad (2.17)$$

where j_0 is the beam current density, and by power balance this must equal the opposite of the power added to the laser field, given approximately by $\Pi \approx cE\Delta E/(2\pi)$ for the low gain regime, where ΔE is the increase in the electric field in one pass through the undulator.

The integral to obtain $P^{(2)}$ cannot be evaluated exactly in closed form, but

assuming that $\psi^{(1)} \ll \psi_0 + Cz$, it can be approximately evaluated to

$$\Pi = j_0 \theta_s E_{ext} l_u \left\langle \int_0^1 \psi^{(1)}(\hat{z}, \psi_0) \sin(\psi_0 + \hat{C}\hat{z}) \, d\hat{z} \right\rangle \qquad (2.18)$$

which gives as the final gain

$$g_s = \frac{2\pi j_0 \theta_s^2 \omega l_u^3}{c\gamma_z^2 \gamma I_A} \left(-2\frac{d}{d\hat{C}} \frac{\sin^2(\hat{C}/2)}{\hat{C}^2} \right) \qquad (2.19)$$

where, recall, l_u is the length of the undulator. This is the gain of the FEL process in the low-gain regime.

2.4 Overview of the Low-Gain Regime

In the low-gain regime, the power output of the FEL grows approximately cubicly with distance along the undulator. This particular model of the low-gain regime requires a monochromatic seeding laser, and accounts for power gain by looking at energy lost from the electron bunch. Although the description above is inadequate to describe high-gain seeded FELs with space charge, it gives a good schematic picture of the behaviour of the electrons in phase space. This intuitive picture can be used as a guide if physical intuition fails in the treatment of the high-gain FELs.

A fundamental assumption was made in the equations of motion in the low-gain regime: the electrons in the bunch do not "talk" to each other. Their dynamics are uncorrelated, as evidenced by the fact that E is taken to be a constant in the equations motion. A proper, complete description of the electron dynamics would take into account the changing laser field due to the

dynamics of the individual electrons. The detailed treatment of this problem, using the self-consistent Maxwell-Vlasov equations, will be the topic of a large part of Chapter 3.

3

An Analytical Model of

Three-Dimensional FELs

I present here an analytical model for free-electron lasers in three dimensions, which follows closely the one dimensional high-gain FEL model presented in [8], and derived by Bonifacio, Pellegrini and Narducci in 1984 [5] using an averaging method, and then derived using a Maxwell-Vlasov treatment by Saldin, Schneidmiller and Yurkov in 1992 [6]. The derivation follows

the Maxwell-Vlasov treatment developed by Saldin, et al. The model is designed to act as a link between analytical models for the CeC pick-up and kicker already developed [9]. The model itself neglects betatron oscillations in the FEL, and considers the transverse dynamics of the electron beam only as a result of the laser field; the transverse dynamics arise purely from Maxwell's equations for the propagation of the laser field. This approach neglects betatron oscillations in the FEL wiggler and transverse space charge effects.

In the first part of this chapter, I present the single-body equations of motion. In the second, I develop the Maxwell-Vlasov instability formalism, and write down the self-consistent equations of motion for this model of FEL amplification. I then solve the problem via Laplace transform, leaving the exact solution in real space in terms of an integral over the Laplace variable and requires the evaluation of the zeros of the dispersion relation, given by

$$ s - \frac{\hat{D}}{1 - \imath\Lambda_p^2 \hat{D}} = 0 $$

The evaluation of $\hat{D}$, which is an integral over the longitudinal energy spread of the electron beam, is discussed at some length in the next chapter, and a closed form series expression for $\hat{D}$ for any $\kappa - N$ distribution is developed, allowing for analysis to any degree of accuracy of the dispersion relation. Finally, all this is put into the context of existing theory with a brief overview of the Green functions for all three phases of coherent electron cooling: pick-up, FEL amplifier, and kicker.

3.1 Single Particle Equations of Motion

I begin by presenting details of results previously published in [10] and [11].

The single-particle hamiltonian for a relativistic particle in an external electromagnetic field is given by

$$\mathcal{H} = c\sqrt{\left(\boldsymbol{p} - \frac{e}{c}\boldsymbol{A}\right)^2 + m^2c^2} + e\phi \tag{3.1}$$

where ϕ is the scalar field, and $\boldsymbol{A}$ is the vector potential. For the purposes of the analysis of FELs, the most convenient independent variable is z, the longitudinal coordinate along the FEL undulator, and therefore it is best to make the change of variables to solve for p_z as

$$p_z = \sqrt{\left(\frac{\mathcal{H}}{c} - \frac{e}{c}\phi\right)^2 - \left(\boldsymbol{p}_\perp - \frac{e}{c}\boldsymbol{A}_\perp\right)^2 - m^2c^2} + \frac{e}{c}A_z \tag{3.2}$$

In the high energy limit, $\mathcal{H}/c$ is large compared to the transverse momentum and mc, and it is therefore convenient to expand the square root as

$$p_z \approx \left(\frac{\mathcal{H}}{c} - \frac{e}{c}\phi\right)\left\{1 - \frac{\left(\boldsymbol{p}_\perp - \frac{e}{c}\boldsymbol{A}_\perp\right)^2 + m^2c^2}{\left(\frac{\mathcal{H}}{c} - \frac{e}{c}\phi\right)^2}\right\} + \frac{e}{c}A_z \tag{3.3}$$

From an appropriate choice of gauge transformation[1], it is always possible to make $\phi = 0$, which leads to the final approximate longitudinal momentum

$$p_z \approx \left(\frac{\mathcal{H}}{c}\right)\left\{1 - \frac{\left(\boldsymbol{p}_\perp - \frac{e}{c}\boldsymbol{A}_\perp\right)^2 + m^2c^2}{(\mathcal{H}/c)^2}\right\} + \frac{e}{c}A_z \tag{3.4}$$

---

[1]See Appendix B

17

First, I break down $\boldsymbol{A}_\perp = \boldsymbol{A}_w + \boldsymbol{A}_l$ where $\boldsymbol{A}_l$ is the laser field, and is in general much smaller in magnitude than $\boldsymbol{A}_w$. This allows the numerator to be linearized in $\boldsymbol{A}_l$. Furthermore, I take $\boldsymbol{p}_\perp = 0$, which implies that

$$v_\perp = c\frac{K}{\gamma_0}(\hat{e}_x \cos k_w z - \hat{e}_y \sin k_w z) \tag{3.5}$$

This approximation requires that the transverse velocity distribution be cold for the electron beam. Under this linearized approximation, the new generator for translation is given by

$$p_z \approx \left(\frac{\mathcal{H}}{c}\right)\left\{1 - \frac{1}{2}\frac{\left(\frac{e}{c}\right)^2\left(\boldsymbol{A}_w^2 + 2\boldsymbol{A}_w \cdot \boldsymbol{A}_l\right) + m^2c^2}{(\mathcal{H}/c)^2}\right\} + \frac{e}{c}A_z \tag{3.6}$$

At this point, we consider an electron beam where the relative energy spread is small, and therefore we define $\mathcal{H} = \mathcal{E}_0 + \mathcal{E}$ and expand to terms quadratic in $\mathcal{E}$. Furthermore, assuming $|\boldsymbol{A}_l| << |\boldsymbol{A}_w|$, I linearize the longitudinal momentum, and thereby obtain

$$p_z \approx \frac{\mathcal{E}_0 + \mathcal{E}}{c} - \frac{1}{2}\frac{1}{\mathcal{E}_0 c}\left(1 - \frac{\mathcal{E}}{\mathcal{E}_0} + \left(\frac{\mathcal{E}}{\mathcal{E}_0}\right)^2\right)\left\{\frac{e^2}{c^2}(\boldsymbol{A}_w^2 + 2\boldsymbol{A}_w \cdot \boldsymbol{A}_l) + m^2c^2\right\} + \frac{e}{c}A_z \tag{3.7}$$

For the equations of motion wherein z is taken as the "time" coordinate, this p_z acts analogously to the hamiltonian. It is the generator of longitudinal translations.

In this one-dimensional model only the energy and time of flight equations [2] are of interest. Taking the relevant derivatives, and considering the energy

---

[2]See Appendix C for a discussion of canonical equations of motion and canonical coordinate transformations.

deviation variable instead of the energy gives

$$\frac{d\mathcal{E}}{dz} = \frac{1}{\mathcal{E}_0 c}\left(1 - \frac{\mathcal{E}}{\mathcal{E}_0} + \mathcal{O}(\mathcal{E}/\mathcal{E}_0)^2\right)\frac{e^2}{c^2}\boldsymbol{A}_w \cdot \frac{\partial \boldsymbol{A}_l}{\partial t} - \frac{e}{c}\frac{\partial A_z}{\partial t} \tag{3.8a}$$

$$\frac{dt}{dz} = \frac{1}{c} - \frac{1}{2}\frac{1}{\mathcal{E}_0 c}\left(-\frac{1}{\mathcal{E}_0} + 2\frac{\mathcal{E}}{\mathcal{E}_0^2}\right)\left\{\left(\frac{e}{c}\boldsymbol{A}_w\right)^2 + m^2 c^2 + 2\frac{e^2}{c^2}\boldsymbol{A}_w \cdot \boldsymbol{A}_l\right\} \tag{3.8b}$$

The set of equations 3.8a and 3.8b determine the longitudinal dynamics in the FEL, and will be revisited and utilized in section 4, when the linearized Maxwell-Vlasov equation is considered and solved.

3.2 Maxwell Equations

From the equations just derived, it is clear that Maxwell equations for $\partial_t \boldsymbol{A}_l$ and $\partial_t A_z$ must be developed. I begin with the transverse laser field, then turn to the longitudinal field. The transverse equations provide a requirement on the definitions of the Fourier transforms to be utilized for the coupled Maxwell-Vlasov equation presented in the next section.

The transverse Maxwell wave equation for the laser field is given by

$$\left(\partial_z^2 - \frac{1}{c^2}\partial_t^2 + \nabla_\perp^2\right)\boldsymbol{A}_l = \frac{4\pi}{c}\boldsymbol{j}_\perp \tag{3.9}$$

where $\boldsymbol{j}_\perp$ is the perpendicular current, which comes from the helical oscillations of the electrons in the undulator field. The laser field is assumed to oscillate close to the resonance frequency, so it is convenient to introduce the Fourier

transformed laser field by

$$\boldsymbol{A}_l(z, t, \boldsymbol{r}_\perp) = \frac{1}{(\sqrt{2\pi})^3} \int d\nu \ d^2k_\perp \ e^{\imath \nu \omega_r (z/c - t)} e^{\imath \boldsymbol{k}_\perp \cdot \boldsymbol{r}_\perp} \tilde{A}_l(\nu, z, \boldsymbol{k}_\perp) \qquad (3.10)$$

The envelope function will generally by slowly varying compared to the laser wavelength, so that

$$\mid \frac{2\nu \omega_r}{c} \partial_z \tilde{A}_l \mid \gg \mid \partial_z^2 \tilde{A}_l \mid$$

In this slowly varying envelope approximation, the Maxwell equation for the envelope equation reads

$$\frac{1}{(\sqrt{2\pi})^3} \int d\nu \ d^2k_\perp \ e^{\imath \nu \omega_r (z/c - t)} e^{\imath \boldsymbol{k}_\perp \cdot \boldsymbol{r}_\perp} \left(2\imath \nu \omega_r / c \ \partial_z \tilde{A}_l - k_\perp^2 \tilde{A}_l \right) = \frac{4\pi}{c} \boldsymbol{j}_\perp \quad (3.11)$$

The transverse current can be related to the longitudinal current by

$$\boldsymbol{j}_\perp = \frac{K}{\gamma_0} \begin{pmatrix} \cos k_w z \\ -\sin k_w z \end{pmatrix} j_z$$

where the longitudinal current is given approximately by

$$j_z \approx -ec \int d\mathcal{E} \ f(z, t, \boldsymbol{r}_\perp, \mathcal{E})$$

where f is the phase space density to be solved for in the Maxwell-Vlasov equation. Using this information, I define the Fourier transform of j_z, which by proxy defines the Fourier transform on f, to be

$$j_z = \frac{1}{(\sqrt{2\pi})^3} \int d\nu \ d^2k_\perp e^{\imath k_w z + \imath \nu \omega_r (z/c - t)} e^{\imath \boldsymbol{k}_\perp \cdot \boldsymbol{r}_\perp} e^{-\imath c k_\perp^2 / (2\nu \omega_r) z} \tilde{j}_z \qquad (3.12)$$

The ponderomotive phase ψ, introduced from considerations of the energy exchange equation in Chapter 2, has arisen this time in the Maxwell equations. By dropping rapidly oscillating terms[3] the transverse Maxwell equation becomes in Fourier space

$$-\frac{2\imath\nu\omega_r}{c}\frac{d}{dz}\left[e^{\imath\frac{ck_\perp^2}{2\nu\omega_r}z}\tilde{A}_\perp\right] = \frac{4\pi}{c}\frac{K}{\gamma_0}\tilde{j}_z \qquad (3.13)$$

The oscillating term whose phase goes as $k_\perp^2 z$ is the source of diffraction effects, and will appear later in the dispersion relation for the transversely infinite beam.

The solution of this gives for the laser field

$$\boldsymbol{A}_w \cdot \tilde{A}_l = e^{-\imath\frac{ck_\perp^2}{2\nu\omega_r}z}e^{\imath k_w z}\left\{\boldsymbol{A}_w \cdot \tilde{A}_l \mid_{z=0} + \frac{\imath\pi}{\nu\omega_r}\frac{K}{\gamma_0}A_w\int_0^z \tilde{j}_z dz'\right\} \qquad (3.14)$$

It is relevant to solve for $\boldsymbol{A}_w \cdot \tilde{A}_l$ as that is the term which appears in the single-particle equations **??**, to within a factor of $\imath\nu\omega_r$.

The longitudinal component of the vector potential accounts for longitudinal space charge effects. From the definition of the electric field in terms of the vector potential (recall that the scalar potential has been made zero by gauge transformation) has the equation

$$E_z = -\frac{1}{c}\frac{\partial A_z}{\partial t}$$

so that the last term of equation 3.8a is just $-eE_z$, which is of course the

---

[3]In this context, rapidly oscillating terms are terms which vary from the ponderomotive phase by $\pm k_w z$. This is equivalent to averaging over one wiggler period.

energy deposited into a given electron by the longitudinal electric field. From Maxwell's equations

$$\partial_t E_z = -\frac{4\pi}{c} j_z$$

so that imposing an identical Fourier transform on E_z as for j_z gives

$$\tilde{E}_z = -\frac{4\pi i}{c\nu\omega_r} \tilde{j}_z \tag{3.15}$$

This solves for all the required terms in the single-particle equations **??**, and can now be combined to generate the coupled Maxwell-Vlasov equation.

3.3 Coupled Maxwell-Vlasov Equation

The Vlasov equation was initially developed to study perturbations to a collisionless plasma [12], and is the standard method for studying instabilities in many-particle systems. In this treatment, the Vlasov equation is effectively one-dimensional, while the three-dimensional effects arise purely from the transverse spread of the laser field and space charge. Assuming the absence of two-body correlations, the single-particle phase space density must be conserved:

$$\frac{df}{dz} = \frac{\partial f}{\partial z} + t'\frac{\partial f}{\partial t} + \mathcal{E}'\frac{\partial f}{\partial \mathcal{E}} = 0 \tag{3.16}$$

Substituting equations **??** directly gives

$$\frac{\partial f}{\partial z} + \left(\frac{1}{c} - \frac{1}{2}\frac{1}{\mathcal{E}_0 c}\left(-\frac{1}{\mathcal{E}_0} + 2\frac{\mathcal{E}}{\mathcal{E}_0^2}\right)\left\{\left(\frac{e}{c}\boldsymbol{A}_w\right)^2 + m^2c^2 + 2\frac{e^2}{c^2}\boldsymbol{A}_w \cdot \boldsymbol{A}_l\right\}\right)\frac{\partial f}{\partial t} +$$
$$\left(\frac{1}{\mathcal{E}_0 c}\left(1 - \frac{\mathcal{E}}{\mathcal{E}_0}\right)\frac{e^2}{c^2}\boldsymbol{A}_w \cdot \frac{\partial \boldsymbol{A}_l}{\partial t} - \frac{e}{c}\frac{\partial A_z}{\partial t}\right)\frac{\partial f}{\partial \mathcal{E}} = 0$$

It is conventional then to take the case where $f = f_1 + f_0$ where f_0 is the background distribution of the bunch and f_1 is a small perturbation on f_0. Since $\boldsymbol{A}_l \propto f_1$, linearizing the above gives the proper linearized Maxwell-Vlasov equation

$$\frac{\partial f_1}{\partial z} + \left(\frac{1}{c} - \frac{1}{2} \frac{1}{\mathcal{E}_0 c} \left(-\frac{1}{\mathcal{E}_0} + 2\frac{\mathcal{E}}{\mathcal{E}_0^2} \right) \left\{ \left(\frac{e}{c} \boldsymbol{A}_w \right)^2 + m^2 c^2 \right\} \right) \frac{\partial f_1}{\partial t} + $$
$$\frac{1}{c} \left(\frac{1}{\mathcal{E}_0} \left(1 - \frac{\mathcal{E}}{\mathcal{E}_0} \right) \frac{e^2}{c^2} \boldsymbol{A}_w \cdot \frac{\partial \boldsymbol{A}_l}{\partial t} - \frac{e}{c} \frac{\partial A_z}{\partial t} \right) \frac{\partial f_0}{\partial \mathcal{E}} = 0 \qquad (3.17)$$

where it has been assumed that $f_0 = n_0 G(\boldsymbol{r}_\perp) F(\mathcal{E})$, where

$$\int d^2 \boldsymbol{r}_\perp \ G(\boldsymbol{r}_\perp) = 1$$

and

$$\int d\mathcal{E} \ F(\mathcal{E}) = 1$$

fixes the normalization for the bunch distribution. This model only considers an infinitely long bunch, but so far considers the possibility of transverse distribution. However, this transverse distribution must be frozen, i.e. $\boldsymbol{p}_\perp = 0$ for all electrons in the bunch.

The appropriate Fourier transform for the phase space distribution is given by

$$f_1 = \frac{1}{(\sqrt{2\pi})^3} \int d\nu \ d^2 k_\perp \ e^{\imath k_w z + \imath \nu \omega_r (z/c - t)} e^{-\imath \frac{k_\perp^2 c}{2\nu \omega_r} z} e^{\imath \boldsymbol{k}_\perp \cdot \boldsymbol{r}_\perp} \tilde{f}_1 \qquad (3.18)$$

takes the linearized Vlasov equation to

$$
\begin{aligned}
&\left\{ \frac{1}{(\sqrt{2\pi})^3} \int d\nu \ d^2k_\perp \ e^{\imath k_w z + \imath \nu \omega_r (z/c-t)} e^{-\imath \frac{k_\perp^2 c}{2\nu\omega_r} z} e^{\imath \boldsymbol{k}_\perp \cdot \boldsymbol{r}_\perp} \times \right. \\
&\left. \left(\imath k_w (1-\nu) + \imath 2 \frac{\mathcal{E}}{\mathcal{E}_0} k_w \nu - \imath \frac{k_\perp^2 c}{2\nu\omega_r} + \partial_z \right) \tilde{f}_1 \right\} + \\
&\left(\frac{1}{\mathcal{E}_0 c} \left(1 - \frac{\mathcal{E}}{\mathcal{E}_0} \right) \frac{e^2}{c^2} \boldsymbol{A}_w \cdot \frac{\partial \boldsymbol{A}_l}{\partial t} + e E_z \right) \frac{\partial f_0}{\partial \mathcal{E}} = 0
\end{aligned}
\tag{3.19}
$$

from the definition of the resonance frequency. Substituting in for the values obtained in the previous section for $\tilde{A}_l$ and $\tilde{E}_z$ gives the second component in Fourier space as

$$
\int d\nu \ d^2k_\perp \ d^2k' \ e^{\imath k_w z + \imath \nu \omega_r (z/c-t)} e^{-\imath \frac{k_\perp^2 c}{2\nu\omega_r} z} e^{\imath \boldsymbol{k}_\perp \cdot \boldsymbol{r}_\perp} e^{\imath \boldsymbol{k}' \cdot \boldsymbol{r}_\perp}
$$

$$
\left\{ \frac{1}{\mathcal{E}_0 c} \frac{e^2}{c^2} (-\imath \frac{\nu\omega_r}{c}) \left(\boldsymbol{A}_w \cdot \boldsymbol{A}_l \mid_{z=0} e^{-\imath k_w z} - \imath \frac{\pi K}{\nu\omega_r \gamma_0} \int_0^z \tilde{j}_z dz' \right) - e\tilde{E}_z \right\} n_0 \frac{dF}{d\mathcal{E}} \tilde{G}(\boldsymbol{k}')
$$

$$
\tag{3.20}
$$

where

$$
G(\boldsymbol{r}_\perp) = \frac{1}{(\sqrt{2\pi})^2} \int d^2q \ e^{\imath \boldsymbol{k}' \cdot \boldsymbol{r}_\perp} \tilde{G}(\boldsymbol{k}')
$$

is the Fourier transform of the transverse electron beam profile. For a homogeneous beam, $\tilde{G}(\boldsymbol{q}) = 2\pi\delta(\boldsymbol{q})$ which gives the infinite beam limit to be considered in later sections. To cope with having two Fourier integrals, one

on each side, take the inverse Fourier transform over $\boldsymbol{r}_\perp$ on both terms gives

$$
\left\{ \frac{1}{(\sqrt{2\pi})^4} \int d\nu \ d^2k_\perp d^2r_\perp \ e^{\imath \boldsymbol{q}\cdot\boldsymbol{r}_\perp} e^{\imath k_w z + \imath \nu \omega_r (z/c - t)} e^{-\imath \frac{k_\perp^2 c}{2\nu\omega_r} z} e^{\imath \boldsymbol{k}_\perp \cdot \boldsymbol{r}_\perp} \times \right.
$$

$$
\left. \left(\imath k_w(1 - \nu) + \imath 2 \frac{\mathcal{E}}{\mathcal{E}_0} k_w \nu - \imath \frac{k_\perp^2 c}{2\nu\omega_r} + \partial_z \right) \tilde{f}_1 \right\} +
$$

$$
\left\{ \frac{1}{(\sqrt{2\pi})^6} \int d\nu \ d^2k_\perp \ d^2k' \ d^2r_\perp \ e^{\imath \boldsymbol{q}\cdot\boldsymbol{r}_\perp} e^{\imath k_w z + \imath \nu \omega_r (z/c - t)} e^{-\imath \frac{k_\perp^2 c}{2\nu\omega_r} z} e^{\imath \boldsymbol{k}_\perp \cdot \boldsymbol{r}_\perp} e^{\imath \boldsymbol{k}' \cdot \boldsymbol{r}_\perp} \right.
$$

$$
\left[\frac{1}{\mathcal{E}_0 c} \frac{e^2}{c^2} (-\imath \frac{\nu \omega_r}{c}) \left(\boldsymbol{A}_w \cdot \boldsymbol{A}_l \ |_{z=0} \ e^{-\imath k_w z} - \imath \frac{\pi K}{\nu \omega_r \gamma_0} \int_0^z \tilde{j}_z dz' \right) - \right.
$$

$$
\left. \left. e \tilde{E}_z \right] n_0 \frac{dF}{d\mathcal{E}} \tilde{G}(\boldsymbol{k}') \right\} = 0
$$

$$(3.21)$$

For "clarity" I have included the two separate integral terms in the separate curly braces. The inverse Fourier transform is taken because it retrieves delta functions out of the individual $\boldsymbol{k}_\perp$, $\boldsymbol{k}'$ and $\boldsymbol{q}$ components, and turns the second set of curly braces into an integral over the kernel given by $\tilde{G}(\boldsymbol{k}_\perp - \boldsymbol{q})$, which for infinite beam is a delta function and for finite beam sizes turns the problem into an integral equation. The former will be focussed upon in the coming sections, while I will return to the issue of finite beam size in a later section.

Resolving these delta functions[4] gives the form for the Maxwell-Vlasov equation

$$
e^{-\imath \frac{k_\perp^2 c}{2\nu\omega_r} z} \left[\imath \left(k_w(1 - \nu) + 2 \frac{\mathcal{E}}{\mathcal{E}_0} k_w \nu - \frac{k_\perp^2 c}{2\nu\omega_r} \right) + \partial_z \right] \tilde{f}_1 =
$$

$$
\int d^2q \ e^{-\imath \frac{q^2 c}{2\nu\omega_r} z} \left[\frac{\imath \nu \omega_r}{\nu \mathcal{E}_0} \frac{e^2}{c^2} \left(\mathcal{U}_0 - \imath \frac{\pi K}{\nu \omega_r \gamma_0} \int_0^z \tilde{j}_z(q) dz' \right) + e \frac{4\pi \imath}{c\nu\omega_r} \tilde{j}_z(q) \right] \times \quad (3.22)
$$

$$
n_0 \frac{dF}{d\mathcal{E}} \tilde{G}(\boldsymbol{k}_\perp - \boldsymbol{q})
$$

---

[4]See Appendix C for a discussion of resolving these delta functions, as well as a discussion of integral equations.

Pausing for a moment, let's consider each term from a physical standpoint. The exponential terms represent the diffraction effects of the laser field propagation through the wiggler. The first term in the braces of the derivative is the phase factor that includes effects from energy spread (the $\mathcal{E}$ term), and a detuning term that arises both from frequency spread (the term proportional to $(1 - \nu)$) in the initial seeding, and the detuning caused by the physical spread of the initial signal (the $k_\perp^2$ term). On the other side of equality, the $\mathcal{U}_0 = \mathbf{A}_w(z) \cdot \mathbf{A}_l \mid_{z=0} e^{-\imath k_w z}$ is a constant after dropping fast oscillating terms, and is the initial source term for a laser field seeding. The term next to it is amplification from the laser field generated by everything in the amplified signal from the beginning of the wiggler to the point z. This integral over the signal that comes before the current point in z is the origin of the exponential amplification. The space charge term arises from the local tendency of the electrons to repel each other when they begin to microbunch. The $dF/d\mathcal{E}$ term contains all the thermal effects, and $\tilde{G}(\mathbf{k}_\perp - \mathbf{q})$ is the symmetric kernel that contains the information about the electron beam's transverse density. In a sense, it accounts for a continuously varying dielectric constant.

Solving this differential equation for $\tilde{f}_1$ is straightforward using an integrating factor, and gives

$$\tilde{f}_1 = e^{-\imath \left(k_w (1-\nu) + 2 k_w \nu \mathcal{E}/\mathcal{E}_0 - k_\perp^2 c/2\nu\omega_r \right) z} \tilde{f}_1 \mid_0 +$$

$$\int_0^z dz' \; e^{\imath \left(k_w (1-\nu) + 2 k_w \nu \mathcal{E}/\mathcal{E}_0 - k_\perp^2 c/2\nu\omega_r \right)(z'-z)} \int d^2 q \; e^{-\imath \frac{(q^2 - k_\perp^2)c}{2\nu\omega_r} z'} \times \quad (3.23)$$

$$\left\{ \frac{\imath \nu \omega_r}{\mathcal{E}_0 c} \frac{e^2}{c^2} \left(\mathcal{U}_0 - \frac{\imath \pi K}{\nu \omega_r \gamma_0} \int_0^{z'} dz'' \; \tilde{j}_z \right) - e \frac{4\pi\imath}{c\nu\omega_r} \tilde{j}_z \right\} n_0 \frac{dF}{d\mathcal{E}} \tilde{G}(\mathbf{q} - \mathbf{k}_\perp)$$

At this point, it is convenient to introduce the *gain length*, Γ^{-1} and the *Pierce parameter*, ρ, which are the natural length and energy scales of the high-gain free electron laser. Taking $\Gamma z = \hat{z}$ and $\rho = \Gamma^{-1} k_w$, and fixing Γ^{-1} to take out the most physical constants, the above equation can be taken dimensionless. These terms will be defined when a natural definition is arrived at in the derivation.

First, consider the phase term, so that defining $\hat{C} = k_w \Gamma^{-1}(1 - \nu) = (1 - \nu)/\rho$ as the normalized detuning parameter, the normalized energy spread by $\hat{\mathcal{E}} = 2\nu \mathcal{E}/\rho \mathcal{E}_0$, and the normalized k-vector by $\hat{k}^2 = k^2 c \Gamma^{-1}/2\nu \omega_r$ fixes all the relevant scales. It is worth noting that for the purposes of the inverse Fourier transform into real $(z, t, \boldsymbol{r}_\perp)$ space, the important values of ν will only vary on the order of ρ from unity[5]. Since for most FELs $\rho \sim .01$, ν is effectively constant, so including it in the normalization causes no mathematical complications. The transverse length scale is determined by the constant

$$\ell^2 = \frac{c\Gamma^{-1}}{(2\nu \omega_r)} \sim 1/\Gamma k_r$$

To give an example here, for an optical wavelength FEL similar to the one to be utilized in eRHIC, a typical gain length will be on the order of 2 meters, while $\lambda_r \sim 5$ μm, so that $\ell^2 \approx 167 \times 10^{-4}$ cm^2 or $\ell \approx 1.2$ mm.

It is now important to properly normalize the energy spread function. From

---

[5]As we will see, the bandwidth of a high-gain FEL is determined by the width of its dispersion relation roots as a function of $\hat{C}$. The real parts of the dispersion relation vary on the order of unity with $\hat{C}$, and therefore with the order of ρ. This will be developed in much greater detail in the next sections.

the previous normalization condition, it is required that

$$\int F d\mathcal{E} = \int \hat{F} d\hat{\mathcal{E}} = \int \hat{F} \frac{2\nu}{\rho \mathcal{E}_0} d\mathcal{E}$$

which clearly suggests for the preservation of normalization that $\hat{F} = (\rho \mathcal{E}_0)/(2\nu)F$. The transverse Fourier distribution can be directly normalized, but contributes no major changes to the normalization of the transverse energy distribution as $d^2 k_\perp \; \tilde{G}$ and $d^2 \hat{k}_\perp \; \hat{G}$ appear as products, so any changes in normalization cancel.

Integrating over the energy $\mathcal{E}$ to obtain a current equation gives the new equation of motion as

$$\tilde{j}_z = -ec \int d\mathcal{E} \; e^{-\imath \left(k_w(1-\nu) + 2k_w \nu \mathcal{E}/\mathcal{E}_0 - k_\perp^2 c/2\nu\omega_r \right)z} \tilde{f}_1 \big|_0 +$$

$$-ec \int d\mathcal{E} \int_0^z dz' \; e^{\imath \left(k_w(1-\nu) + 2k_w \nu \mathcal{E}/\mathcal{E}_0 - k_\perp^2 c/2\nu\omega_r \right)(z'-z)} \int d^2 q \; e^{-\imath \frac{(q^2 - k_\perp^2)c}{2\nu\omega_r} z'} \times$$

$$\left\{ \frac{\imath \nu \omega_r}{\mathcal{E}_0 c} \frac{e^2}{c^2} \left(\mathcal{U}_0 - \frac{\imath \pi K}{\nu \omega_r \gamma_0} \int_0^{z'} dz'' \; \tilde{j}_z \right) - e \frac{4\pi \imath}{c\nu\omega_r} \tilde{j}_z \right\} n_0 \frac{dF}{d\mathcal{E}} \tilde{G}(\boldsymbol{q} - \boldsymbol{k}_\perp)$$

$$(3.24)$$

Introducing the properly normalized coordinates and setting the normalization so that the coefficient of $\imath \int dz'' \tilde{j}_z$ is unity requires that the gain length be given by

$$\Gamma^{-1} = \left(\frac{\mathcal{E}_0^2 c^2 \gamma_0}{2\pi \nu e^3 K k_w n_0} \right)^{1/3}$$

and the space charge parameter be defined as

$$\hat{\Lambda}_p^2 = \frac{8\pi e^2 n_0 \Gamma^{-1}(1 + K^2)}{\gamma_0^3 m c^3}$$

28

so that the final integral equation for the longitudinal current distribution be given by

$$\tilde{j}_z = -ec\frac{\rho\mathcal{E}_0}{2\nu}\int d\hat{\mathcal{E}}\ e^{\imath(\hat{C}+\hat{\mathcal{E}}-\hat{k}_\perp^2)\hat{z}}\tilde{f}_1\mid_{\hat{z}=0} +$$

$$\int d\hat{\mathcal{E}}\int_0^{\hat{z}} d\hat{z}' e^{\imath(\hat{C}+\hat{\mathcal{E}}-\hat{k}_\perp^2)(\hat{z}'-\hat{z})}\int d^2\hat{q}\ e^{-\imath(\hat{q}^2-\hat{k}_\perp^2)\hat{z}'}\times \tag{3.25}$$

$$\left\{\hat{\mathcal{U}}_0 + \int_0^{\hat{z}'} d\hat{z}''\ \tilde{j}_z + \imath\hat{\Lambda}_p^2\tilde{j}_z\right\}\frac{d\hat{F}}{d\hat{\mathcal{E}}}\hat{G}(\boldsymbol{q}-\boldsymbol{k}_\perp)$$

From this point there are two avenues to consider: the case of infinite beam and the case of finite beam. Switching to normalized coordinates follows a similar procedure in both cases, but in the finite beam case the integral equation remains, and must be considered using a formalism that generalizes the simpler infinite beam case. Since the infinite beam case is mathematically easier to consider, and is of interest for the CeC model being developed, I consider that case first. The finite beam case is left for the next section.

3.4 Infinite Beam

For comparison to the work in [9] regarding Debye screening, I consider the limit of an infinite beam. In this case, $\hat{G}(\boldsymbol{q}-\boldsymbol{k}_\perp) = \delta(\boldsymbol{q}-\boldsymbol{k}_\perp)$ and the integral equation simplifies greatly.

3.4.1 Solution by Laplace Transform

Taking the infinite beam case removes the $\hat{q}$ integration and leaves the integral equation for the current given by:

$$\tilde{j}_z = -ec\frac{\rho\mathcal{E}_0}{2\nu}\int d\hat{\mathcal{E}}\ e^{\imath(\hat{C}+\hat{\mathcal{E}}-\hat{k}_\perp^2)\hat{z}}\tilde{f}_1\mid_{\hat{z}=0}\ +$$

$$\int_0^{\hat{z}}d\hat{z}'\left\{\hat{\mathcal{U}}_0+\int_0^{\hat{z}'}d\hat{z}''\ \tilde{j}_z+\imath\hat{\Lambda}_p^2\tilde{j}_z\right\}\int d\hat{\mathcal{E}}\ \frac{d\hat{F}}{d\hat{\mathcal{E}}}e^{\imath(\hat{C}+\hat{\mathcal{E}}-\hat{k}_\perp^2)(\hat{z}'-\hat{z})} \tag{3.26}$$

By happy coincidence, this equation can be solved by a Laplace transform in the $\hat{z}$ variable[6] which yields the solution of the initial value problem in Laplace transformed space as

$$J(s)=\frac{-ec\frac{\rho\mathcal{E}_0}{2\nu}\int d\hat{\mathcal{E}}\ \frac{1}{s+\imath(\hat{C}+\hat{\mathcal{E}}-\hat{k}_\perp^2)}\tilde{f}_1\mid_{\hat{z}=0}\ +\hat{D}\ \hat{\mathcal{U}}_0}{1-\left(\frac{1}{s}+\imath\hat{\Lambda}_p^2\right)\hat{D}} \tag{3.27}$$

where

$$\hat{D}=\int d\hat{\mathcal{E}}\ \frac{d\hat{F}}{d\hat{\mathcal{E}}}\frac{1}{s+\imath(\hat{C}+\hat{\mathcal{E}}-\hat{k}_\perp^2)} \tag{3.28}$$

As discussed in the Appendix, the dispersion relation is related to the zeros of the denominator, which are solutions to the equation

$$s=\frac{\hat{D}}{1-\imath\hat{\Lambda}_p^2\hat{D}} \tag{3.29}$$

Once these poles are known, the solution can be straightforwardly solved from the inverse Laplace transform. I will explore the exact evaluation of the dispersion relation in the next chapter.

---

[6]see Appendix C for a detailed discussion of these Laplace transforms.

3.4.2 Green Function for Infinite Beam

I am now in a position to write the solution to the initial value problem as a triple integral. Looking back at equation 3.27 it is possible to write the series as a sum over the poles of the dispersion relation in the denominator, *i. e.*

$$\tilde{j}_z = -ec\frac{\rho\mathcal{E}_0}{2\nu}\sum_{j}\int d\hat{\mathcal{E}}\ \frac{s_j e^{s_j\hat{z}}}{1 - \hat{D}'_j + i\hat{\Lambda}_p^2\left(\hat{D}_j + s_j\hat{D}'_j\right)}\frac{1}{s_j + i(\hat{C} + \hat{\mathcal{E}} - \hat{k}_\perp^2)}\tilde{f}_1\mid_{\hat{z}=0}$$

(3.30)

where s_j is a root of the dispersion relation, $\hat{D}_j$ is the value of $\hat{D}$ at the s_j root, and $\hat{D}'$ is the derivative with respect to s. I have dropped the oscillating/decaying mode that arises from the $s + i(\hat{C} + \hat{\mathcal{E}} - \hat{k}_\perp^2)$ root that is non-degenerate with the dispersion roots. The initial seeding field $\mathcal{U}_0$ has also been dropped as it plays no role in CeC.

Capturing all of the roots in the dispersion relation is necessary for numerical analysis, as it is necessary to be very careful near these points. At a degeneracy point such as the two-fold degeneracy between the growing and decaying roots in figure 4.1, the degeneracy arises in the form of a derivative with respect to s at that point. For thermal cases it can be seen that the problem does not arise, as the thermal effects lift the degeneracy.

In any case, for applications to CeC we desire the Green function, which is obtained by considering the case of

$$f_1\mid_0 = \frac{2\nu}{\rho\mathcal{E}_0}\delta(t - t_0)\delta(\hat{\mathcal{E}} - \hat{\mathcal{E}}_0)\delta(\boldsymbol{r}_\perp - \boldsymbol{r}_{\perp 0})$$

where the normalization accounts properly for going from some initial energy

deviation E_0 into the normalized variables. Applying the original definition of the Fourier transform, and using the proper choice of normalized variables gives

$$\tilde{f}_1 \mid_0 = \frac{1}{\sqrt{2\pi}^3} \frac{2\nu}{\rho \mathcal{E}_0} e^{-i\hat{k}_\perp \cdot \hat{r}_{\perp 0}} e^{i(1-\rho\hat{C})\omega_r t_0} \delta(\hat{\mathcal{E}} - \hat{\mathcal{E}}_0)$$

Inserting this into the integral above gives the Green function for the current distribution[7]

$$\mathcal{G}(\hat{r}_{\perp 0}, t_0, \hat{\mathcal{E}}_0) = -ec \frac{1}{\sqrt{2\pi}^3} \sum_j \frac{s_j e^{s_j \hat{z}}}{1 - \hat{D}'_j + i\hat{\Lambda}_p^2 \left(\hat{D}_j + s_j \hat{D}'_j\right)} \times$$
$$\frac{1}{s_j + i(\hat{C} + \hat{\mathcal{E}}_0 - \hat{k}_\perp^2)} \left(\frac{1}{\sqrt{2\pi}^3} e^{-i\hat{k}_\perp \cdot \hat{r}_{\perp 0}} e^{i(1-\rho\hat{C})\omega_r t_0}\right) \tag{3.31}$$

where $\hat{k}_\perp \cdot \hat{r}_\perp = k_\perp \cdot r_\perp$ by the choice of normalizing the transverse variable. Given some general initial condition on phase space given by $f_1(r_{\perp 0}, t_0, \hat{\mathcal{E}}_0)$ returns the final current

$$\tilde{j}_z = \int d^2 r_{\perp 0} \, dt_0 \, d\hat{\mathcal{E}}_0 \, \mathcal{G}_{\text{FEL}}(\hat{r}_{\perp 0}, t_0, \hat{\mathcal{E}}_0) \times f_1(r_{\perp 0}, t_0, \hat{\mathcal{E}}_0) \tag{3.32}$$

with proper normalization to be made on the phase space distribution.

From these considerations, and considering equation 3.26, it is straightforward enough to calculate the phase space density Green function. By comparing what is under the energy integral for the current equation to the definition of the current in terms of the phase space density, a Green function for an

---

[7]Obtaining the Green function for the phase space distribution can be obtained by inserting the resulting Fourier transformed current into equation 3.23

arbitrary initial perturbation is given by

$$-ec\tilde{f}_1(\hat{\boldsymbol{k}}_\perp, \hat{C}, \hat{\mathcal{E}}) = e^{\imath(\hat{C}+\hat{\mathcal{E}}-\hat{k}_\perp^2)\hat{z}} \tilde{f}_1 \mid_{\hat{z}=0} (\hat{\boldsymbol{k}}_\perp, \hat{C}, \hat{\mathcal{E}}) +$$

$$\int d^2\hat{\boldsymbol{r}}_{\perp 0} \, dt_0 \int_0^{\hat{z}} d\hat{z}' \; e^{\imath(\hat{C}+\hat{\mathcal{E}}-\hat{k}_\perp^2)(\hat{z}'-\hat{z})} \times \quad (3.33)$$

$$\left\{ \int_0^{\hat{z}'} d\hat{z}'' \; \mathcal{G}(\hat{z}'', \hat{\boldsymbol{r}}_{\perp 0}, t_0, \hat{\mathcal{E}}) + \imath\hat{\Lambda}_p^2 \mathcal{G}(\hat{z}', \hat{\boldsymbol{r}}_{\perp 0}, t_0, \hat{\mathcal{E}}) \right\} \tilde{f}_1 \mid_{\hat{z}=0} (\hat{\boldsymbol{r}}_{\perp 0}, t_0, \hat{\mathcal{E}})$$

where initial laser seeding has been taken to zero and transient oscillatory
terms have been neglected, so that only the FEL amplified process is included
here. Explicitly, this gives the FEL phase space density Green function as

$$\mathcal{G}_{\text{FEL}} = e^{\imath(\hat{C}+\hat{\mathcal{E}}-\hat{k}_\perp^2)\hat{z}} +$$

$$\sum_{\jmath} \frac{1}{1 - \hat{D}_{\jmath}' + \imath\hat{\Lambda}_p^2 \left(\hat{D}_{\jmath} + s_{\jmath}\hat{D}_{\jmath}' \right)} \left(\frac{1}{s_{\jmath} + \imath(\hat{C} + \hat{\mathcal{E}}_0 - \hat{k}_\perp^2)} \right)^2 \times$$

$$\left\{ (1 + \imath\hat{\Lambda}_p^2 s_{\jmath}) \left[\left(e^{s_{\jmath}\hat{z}} - e^{-\imath(\hat{C}+\hat{\mathcal{E}}_0-\hat{k}_\perp^2)\hat{z}} \right) - \left(1 - e^{-\imath(\hat{C}+\hat{\mathcal{E}}_0-\hat{k}_\perp^2)\hat{z}} \right) \right] \right\} \frac{d\hat{F}}{d\hat{\mathcal{E}}_0}$$

$$\times e^{-\imath\hat{k}_\perp \cdot \hat{r}_{\perp 0}} e^{\imath(1-\rho\hat{C})\omega_r t_0} \delta(\hat{\mathcal{E}} - \hat{\mathcal{E}}_0)$$

so that the final phase space distribution given an initial phase space distri-
bution is given by

$$\tilde{f}_1(\hat{C}, \hat{\mathcal{E}}, \hat{\boldsymbol{k}}_\perp) = \int d^2\hat{\boldsymbol{r}}_{\perp 0} \, dt_0 \; \mathcal{G}_{\text{FEL}}(\hat{C}, \hat{\boldsymbol{k}}_\perp, \hat{\mathcal{E}}; \hat{\boldsymbol{r}}_{\perp 0}, t_0, \hat{\mathcal{E}}_0) \times \tilde{f}_1 \mid_{\hat{z}=0} (\hat{\boldsymbol{r}}_{\perp 0}, t_0, \hat{\mathcal{E}}_0)$$

$$(3.35)$$

3.5 Finite Beam Size

Equation 3.26 is sufficiently general to solve for an arbitrary transverse distribution. In all but the infinite beam case, the Fourier transform of the transverse beam profile behaves as a kernel in an integral equation, which is best solved by an expansion in eigenmodes of the kernel.

3.5.1 Mode Expansion

The correct expansion[8] to consider for the integral equation is in terms of the integral of the Fourier transformed current density

$$\int_0^{\hat{z}} d\hat{z}' \, \tilde{j}_z(\hat{z}') = \sum_\ell \psi_\ell(\boldsymbol{k}_\perp) e^{\imath \boldsymbol{k}_\perp^2 \hat{z}} a_\ell(\hat{z}) \tag{3.36}$$

where the a_ℓ contains the exponential growth or decay of a given mode. Here the eigenmodes satisfy the equation

$$\psi_\ell(\boldsymbol{k}_\perp) = \frac{1}{\omega_\ell} \int d^2 q_\perp \, \hat{G}(\boldsymbol{k}_\perp - \boldsymbol{q}_\perp) \psi_\ell(\boldsymbol{q}_\perp) \tag{3.37}$$

for some eigenvalue ω_ℓ. Because $G(\boldsymbol{r}_\perp)$ is a smooth real function, its Fourier transform is hermitian, therefore ω_ℓ is real and the eigenvectors are orthogonal. Because the basis for these kernels are countable, a matrix expansion for the eigenmodes is possible, which I will exploit later.

Inserting this definition for the expansion of $\int d\hat{z}' \tilde{j}_z$ into equation 3.26 gives

---

[8]Reprinted excerpt with permission from S. Webb, G. Wang and V. Litvinenko, PRST-AB, Accepted for publication. Copyright (2011) by the American Physical Society.

a matrix expansion of the a_i for each mode as

$$
\begin{aligned}
a'_\ell - \imath Q_{m,\ell} a_m = -ec\frac{\rho \mathcal{E}_0}{2\nu} \int d\hat{\mathcal{E}} \int d^2 \hat{k}_\perp \ e^{\imath(\hat{C}+\hat{\mathcal{E}}-\hat{k}_\perp^2)\hat{z}} \tilde{f}_1 \mid_0 \psi_\ell(\hat{k}_\perp) - \\
\int d\hat{\mathcal{E}} \int_0^{\hat{z}} d\hat{z}' \ e^{\imath(\hat{C}+\hat{\mathcal{E}})(\hat{z}'-\hat{z})} \times \frac{1}{\omega_\ell}\left\{ a_n + \imath \hat{\Lambda}_p^2 \left[a'_\ell + \imath Q_{m,\ell} a_m\right]\right\}\frac{d\hat{F}}{d\hat{\mathcal{E}}}
\end{aligned}
\tag{3.38}
$$

where

$$
Q_{m,\ell} = \int d^2 k_\perp \ k_\perp^2 \psi_m(\boldsymbol{k}_\perp)\psi_\ell(\boldsymbol{k}_\perp) \tag{3.39}
$$

is a measure of the mode coupling. The resulting matrix equation for the a_i may be solved by Laplace transform, which gives in Laplace space

$$
\left[\left(s - \hat{D}\omega_m(1 + \imath s \hat{\Lambda}_p^2)\right)\delta_{\ell,m} + (1 + \imath \hat{\Lambda}_p^2 \omega_m)Q_{\ell,m}\right]a_m = \tilde{f}_1^\ell \tag{3.40}
$$

Solution of this matrix equation requires understanding the matrix elements of $Q_{\ell,m}$, which in turn requires understanding the eigenvectors of the kernel. In general the kernel does not have a closed form set of eigenmodes, so some expansion in a basis of orthonormal special functions is necessary. To illustrate this procedure, I will take as an example the gaussian transverse beam profile.

3.5.2 Gaussian Beam Profile

Take the transverse profile as

$$
G(\boldsymbol{r}_\perp) = \exp\left(-r_\perp^2/2\hat{L}^2\right) \tag{3.41}
$$

Then the eigenvalue equation is given by

$$\psi_\ell(\boldsymbol{k}_\perp) = \frac{1}{\omega_\ell} \int d^2\boldsymbol{q} \; \left(\frac{\hat{L}}{\sqrt{2\pi}}\right)^2 \exp\left\{-\frac{(\boldsymbol{k}_\perp - \boldsymbol{q})^2}{2\hat{L}^{-2}}\right\} \psi_\ell(\boldsymbol{q}) \qquad (3.42)$$

This is separable in cartesian coordinates such that

$$\psi_\ell(\boldsymbol{p}) = \chi_m(p_x)\chi_n(p_y) \qquad (3.43)$$

which then satisfies independent eigenvalue equations

$$\chi_m(p_\imath) = \frac{1}{\lambda_m} \int_{-\infty}^{\infty} dp'_\imath \; \frac{\hat{L}}{\sqrt{2\pi}} \exp\left\{-(p_\imath^2 + p_\imath'^2 - 2p_\imath p'_\imath)/2\hat{L}^{-2}\right\} \chi_m(p'_\imath) \qquad (3.44)$$

where the resulting eigenvalue for ψ_ℓ is given by $\omega_\ell = \lambda_n \lambda_m$. It is convenient to define the normalized variable $\mu = p_\imath \hat{L}$ so that the above eigenvalue equation is given by

$$\chi_m(\mu) = \frac{1}{\hat{\lambda}_m} \int_{-\infty}^{\infty} d\mu' \; \exp\left\{-(\mu^2 + \mu'^2 - 2\mu\mu')/2\right\} \chi_m(\mu') \qquad (3.45)$$

where $\hat{\lambda}_m = \lambda_m\sqrt{2\pi}$. The appropriate scaling for the transverse beam size for the full eigenvalue is given by

$$\omega_\ell = \frac{\hat{\omega}_\ell}{2\pi}$$

where $\hat{\omega}_\ell = \hat{\lambda}_m \hat{\lambda}_n$. To calculate the normalized eigenvalues, we expand the kernel of this single-variable integral equation in terms of Hermite polynomials, as they are already related to the paraxial Maxwell equations [13].

It turns out from the properties of Hermite polynomials that only the evens

and odds couple, so each χ_m is a series in either even or odd Hermite polynomials. In this case, the matrix equation for the even Hermite polynomials is given approximately by the matrix elements

$$\mathsf{G}_{a,b} = \int_{-\infty}^{\infty} d\mu \int_{-\infty}^{\infty} d\mu' \; \exp\left\{-(\mu^2 + \mu'^2 - 2\mu\mu')/2\right\} \\ H_a(\mu)e^{-\mu^2/2}H_b(\mu')e^{-\mu'^2/2} \tag{3.46}$$

Furthermore, to good approximation, the expansion can be carried out for the first two Hermite functions in the series. We therefore consider the two-mode case. For the principle even mode, the matrix is given by

$$\mathsf{G} = \begin{pmatrix} 2\sqrt{\frac{\pi}{3}} & \frac{1}{3}\sqrt{\frac{2\pi}{3}} \\ \frac{1}{3}\sqrt{\frac{2\pi}{3}} & \sqrt{\frac{\pi}{3}} \end{pmatrix} \tag{3.47}$$

for the vector components $(H_0(\mu), H_2(\mu))^t \exp(-\mu^2/2)$. The eigensystem here has eigenvalue $\hat{\lambda}_{even} = 2.2382$ with corresponding eigenvector

$$\boldsymbol{v}_{even} = \begin{pmatrix} .9294 \\ .3690 \end{pmatrix}$$

and a smaller eigenvalue $\hat{\lambda}_2 = .83178$ with corresponding eigenvector

$$\begin{pmatrix} -.1465 \\ .3690 \end{pmatrix}$$

To validate these numerical results we take the matrix to next order, *i.e.*

to order $H_4(\mu)$ in the expansion, and the matrix is given by

$$
\mathtt{G} = \begin{pmatrix} 2\sqrt{\frac{\pi}{3}} & \frac{1}{3}\sqrt{\frac{2\pi}{3}} & \frac{1}{9}\sqrt{\frac{\pi}{2}} \\ \frac{1}{3}\sqrt{\frac{2\pi}{3}} & \sqrt{\frac{\pi}{3}} & \frac{17}{54}\sqrt{\pi} \\ \frac{1}{9}\sqrt{\frac{\pi}{2}} & \frac{17}{54}\sqrt{\pi} & \frac{227}{324}\sqrt{\frac{\pi}{3}} \end{pmatrix}
\tag{3.48}
$$

which yields an eigensystem given by $\hat{\lambda}_1' = 2.3157$, $\hat{\lambda}_2' = 1.2005$ and $\hat{\lambda}_3' = .27073$ with corresponding normalized eigenvectors

$$
\boldsymbol{v}_1 = \begin{pmatrix} .8772 \\ .4244 \\ .2245 \end{pmatrix}
$$

$$
\boldsymbol{v}_2 = \begin{pmatrix} -.1724 \\ .2376 \\ .2245 \end{pmatrix}
$$

$$
\boldsymbol{v}_3 = \begin{pmatrix} .03343 \\ -.1879 \\ .2245 \end{pmatrix}
$$

We can conclude from this that the largest eigenvalue can be accurately determined to within 3% with the 2×2 matrix expansion, and from analysis of the eigenvector components the $H_4(\mu)$ level of expansion is negligibly small compared to the other two components for the eigenvector with the maximal eigenvalue.

Carrying out a similar procedure for the $H_1(\mu)$ - $H_3(\mu)$ eigenmode gives a

maximal eigenvalue $\hat{\lambda}_{odd} = 1.7161$ and eigenvector

$$\boldsymbol{v}_{odd} = \begin{pmatrix} .8456 \\ .5339 \end{pmatrix}$$

It is now necessary to calculate the various matrix elements for Q. For the purposes orderly book-keeping, we define the following modes

$$\psi_{even} = \chi_{even}(\mu_x)\chi_{even}(\mu_y) \tag{3.49a}$$

$$\psi_{odd} = \chi_{odd}(\mu_x)\chi_{odd}(\mu_y) \tag{3.49b}$$

$$\psi_{+} = \frac{1}{\sqrt{2}}\left(\chi_{odd}(\mu_x)\chi_{even}(\mu_y) + \chi_{even}(\mu_x)\chi_{odd}(\mu_y)\right) \tag{3.49c}$$

$$\psi_{-} = \frac{1}{\sqrt{2}}\left(\chi_{odd}(\mu_x)\chi_{even}(\mu_y) - \chi_{even}(\mu_x)\chi_{odd}(\mu_y)\right) \tag{3.49d}$$

as the orthonormal basis of expansion. The corresponding eigenvalues are given by $\hat{\omega}_{even} = 5.0095$, $\hat{\omega}_{odd} = 2.945$ and $\hat{\omega}_{+} = \hat{\omega}_{-} = 3.8410$. Under this particular basis the Hermite polynomials have a particularly nice relation for the Q matrix elements, and Q is diagonal. The individual modes do not couple, and their growth rates are determined by the dispersion relation

$$\left(s - \hat{D}\omega_m(1 + \imath s\hat{\Lambda}_p^2)\right) + (1 + \imath\hat{\Lambda}_p^2\omega_m)Q_{m,m} = 0 \tag{3.50}$$

The individual Q are given by $Q_{even} = 2.51446/\hat{L}^4$, $Q_{odd} = 6.35275/\hat{L}^4$, and $Q_{+} = Q_{-} = 4.43333/\hat{L}^4$. The growth rate for these parameters is given in figure (3.1)[9], with $\hat{L} = 3$.

---

[9]Reprinted figure with permission from [FULL REFERENCE CITATION] as follows: S.
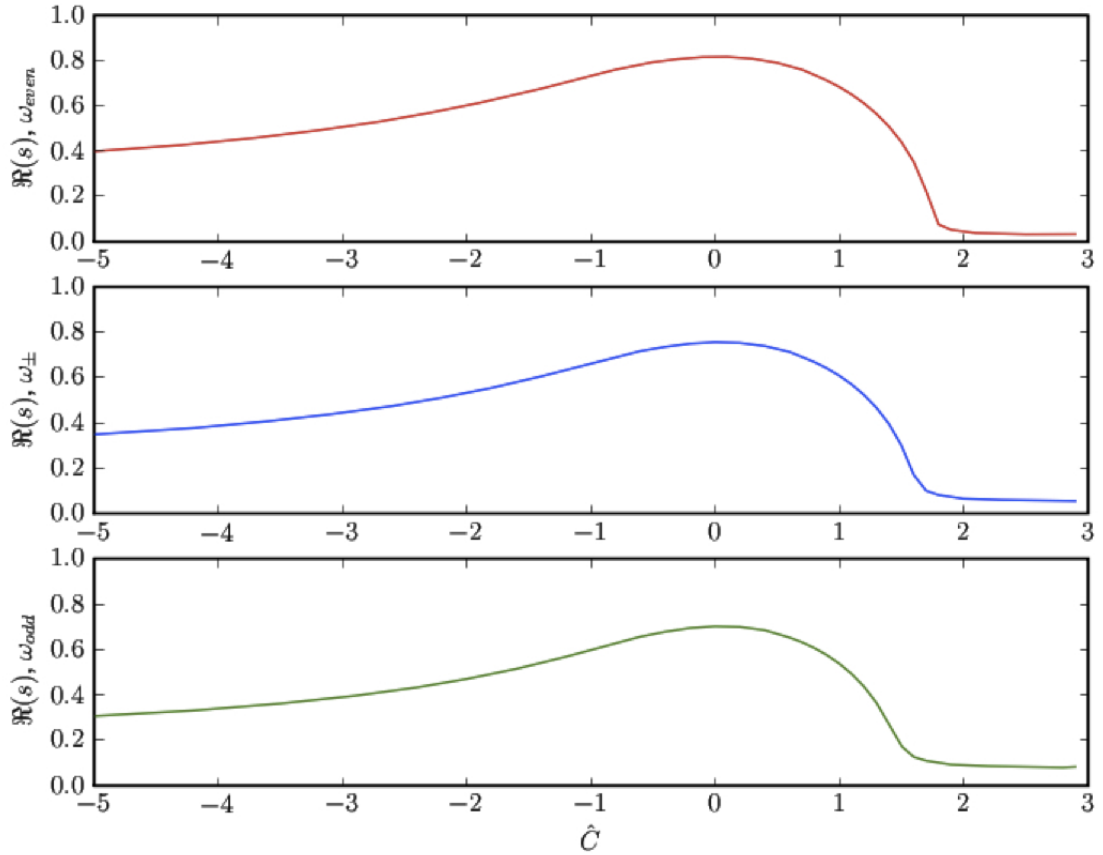
Figure 3.1: Growth rates for three eigenmodes: (i) top is of mode with largest eigenvalue, (ii) is degenerate case of the odd/even mixtures, (iii) is of smallest eigenvalue

40

To recap, we have calculated an eigenbasis for the transverse beam profile, yielding a linear superposition of even- and odd-numbered Hermite polynomials, and their corresponding eigenvalues. The series is truncated at two dominant modes, and because of the particular nature of the Hermite polynomial expansion basis, the Q matrix is diagonal. If Q had off-diagonal matrix elements, there would be "gain leakage" between the connected eigenvectors.

3.5.3 One-Dimensional Limit

Because the eigenvalues are totally independent of the transverse size, and only Q is dependent, it is straightforward to get directly to the one-dimensional beam limit for the dispersion relation. By redefining the normalization as

$$\tilde{s} = s\omega_m^{-1/3} \tag{3.51a}$$

$$\tilde{C} = \hat{C}\omega_m^{-1/3} \tag{3.51b}$$

$$\tilde{\Lambda}_p^2 = \hat{\Lambda}_p^2\omega_m^{1/3} \tag{3.51c}$$

$$\tilde{Q}_m = Q_m\omega_m^{-1/3} \tag{3.51d}$$

the dispersion relation takes the form

$$\tilde{s} - \frac{\imath}{(\tilde{s} + \imath\tilde{C})^2}(1 + \imath\tilde{s}\tilde{\Lambda}_p^2) + (1 + \imath\tilde{\Lambda}_p^2\omega_m^{2/3})\tilde{Q} = 0 \tag{3.52}$$

The actual scaling is such that, for large beams, the portion of this dispersion relation identical in form to the one-dimensional dispersion relation comes to strongly dominate over the perturbation correction for finite size, taken by the value of Q_m. For the case of an infinitely large transverse size all functions are eigenmodes and all all eigenvalues are unity, therefore we can obtain the one-dimensional limit through this limit.

3.6   Conclusion

In this chapter I provided a derivation for a three-dimensional model of the FEL amplification process that considers any arbitrary transverse beam profile and longitudinal energy spread. This model reduces to the one-dimensional limit under appropriate limits of the parameters. This results in a problem that may be solved as a three-dimensional Fourier transform in $(\hat{C}, \boldsymbol{k}_\perp)$ space, and provides a fast-converging mode expansion method for an arbitrary transverse beam profile.

A number of restrictions remain for this model. The foremost is that it neglects transverse momentum spread. This, combined with neglecting betatron oscillations, prevents this model from accounting for the full set of physical effects on the electron bunch dynamics. Future work should find a way to incorporate the transverse motion, probably by some form of averaging under the assumption that the betatron wavelength in the undulator is small compared to FEL gain length. However, for the purposes of benchmarking numerical code, it is reasonable to simply set the input parameters such that this model matches the dynamics being modeled by the code. Thus, as a benchmarking

tool, this model is satisfactory.

4

Dispersion Relations

Evaluating $\hat{D}$ is at the core of evaluating the dispersion relation. Results are analytically known in the published literature [8] for three cases:

1. Cold beam, $\hat{F} = \delta(\hat{P})$

2. Lorentzian beam, $\hat{F} = (\hat{q}/\pi)(\hat{P}^2 + \hat{q}^2)^{-1}$

3. Gaussian beam, $\exp[-\hat{P}^2/2\hat{\Lambda}_T^2]/\sqrt{2\pi\hat{\Lambda}_T^2}$

I present the first two in detail, the first because it provides a necessary limit to test a general expression, and the second because its method of evaluation is instructive for evaluating the general case. The third result is presented without derivation, as it represents the large N limit and due to the function diverging at $\pm\imath\infty$ the integrals cannot be evaluated in the same way as the others. It is merely presented for completeness.

A more general method for evaluating the dispersion relations, as well as the properties of the roots of this dispersion relation, is developed and presented in full detail, having already been published in [14]. In this, I prove that the roots are well-bounded, and furthermore that they converge despite the series for $\hat{D}$ diverging in the approach to the gaussian limit. The methods discussed in this section may be readily applied to other plasma instability problems, as well.

Cold Beam

For a cold beam

$$\hat{D} = \int_{-\infty}^{\infty} d\hat{P} \; \frac{1}{s + \imath(\hat{C} + \hat{P} + \hat{k}_\perp^2)} \frac{d}{d\hat{P}} \delta(\hat{P}) \tag{4.1}$$

By integration by parts, the derivative on the delta function can be moved to the argument, so that it can be found that

$$\hat{D}_{cb} = \frac{\imath}{\left(s + \imath(\hat{C} + \hat{k}_\perp^2)\right)^2} \tag{4.2}$$

45

This gives a cubic equation for the dispersion relation, namely

$$s\left((s + \imath(\hat{C} + \hat{k}_\perp^2))^2 + \hat{\Lambda}_p^2\right) = \imath \tag{4.3}$$

which can be solved in closed form by the Cardano formula. More importantly, it is an important test for the thermal distributions that they all return to this cubic equation when their energy spread parameter goes to zero.

The cold beam roots are given in figure 4.1, where the horizontal axis is the useful parameter $\hat{C}_{3D} = \hat{C} + \hat{k}_\perp^2$. In these graphs, the space charge parameter is set to $\hat{\Lambda}_p^2 = 0$. Notice that there is a cutoff on the exponential growth regime, above which no further growth is possible. This occurs when the bunch wavelength is too long to interact with the oscillations constructively. When space charge is non-zero, there is a cutoff in growth for some value of $\hat{C}$ to the left of the long wavelength cutoff. This short wavelength cutoff occurs when the longitudinal space charge of the charge "sheets" forming in the lasing process causes the "sheets" to repel each other too much, and they cannot grow any further below the critical wavelength.

This result is of interest because it provides the simplest standard on what the roots look like, and because all of the future distributions should limit to these dispersion relations in the zero energy spread limit.

Lorentzian Distribution

For a Lorentzian energy distribution

$$\hat{F} = \frac{\hat{q}}{\pi} \frac{1}{\hat{P}^2 + \hat{q}^2} \tag{4.4}$$
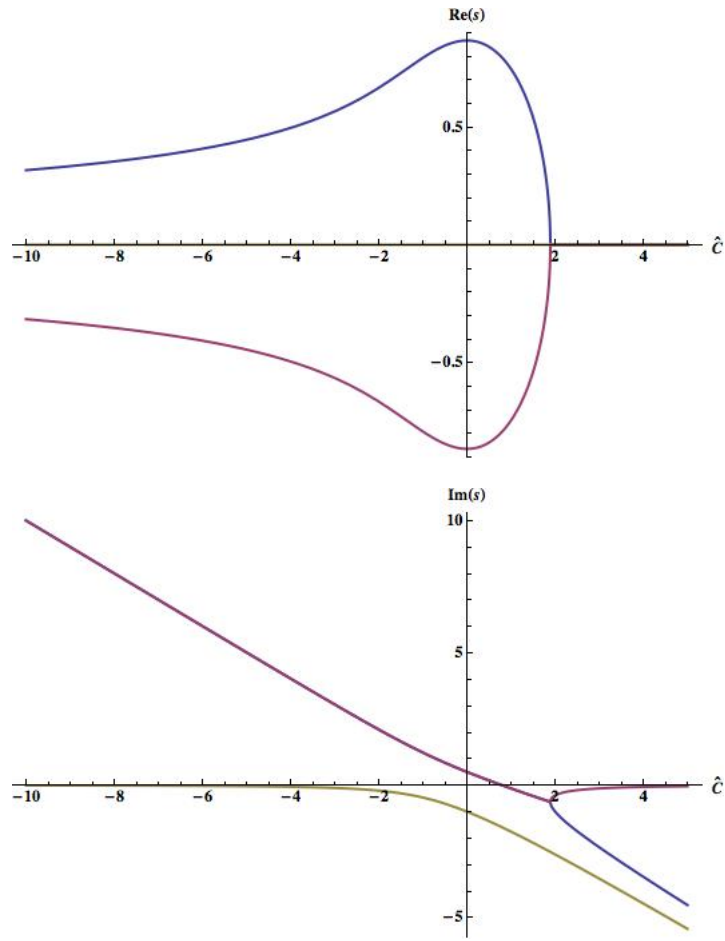
Figure 4.1: Real and imaginary components of the roots for cold beam.
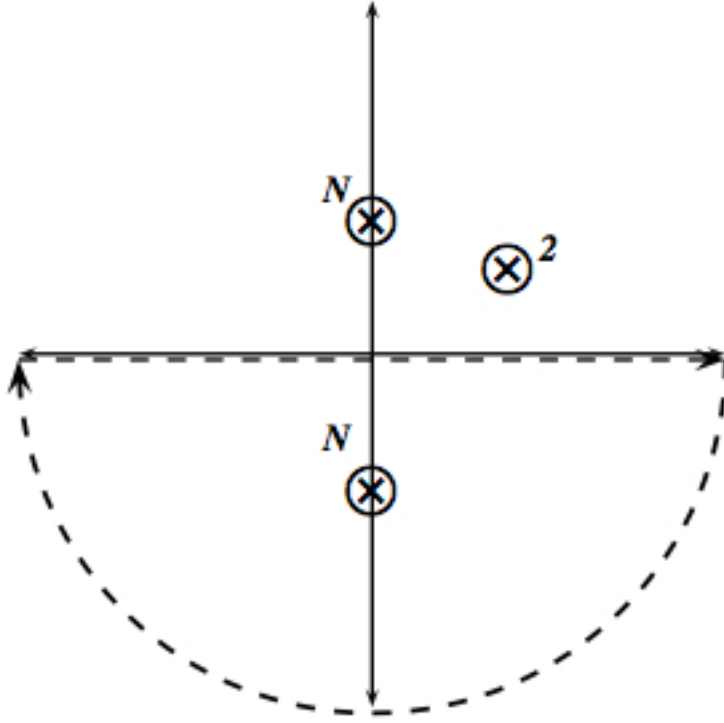
Figure 4.2: Pole structure of the $\hat{D}$ integral.

the integral may be evaluated by looking at the pole structure on the complex $\hat{P}$-plane of the functions. There are poles at $\pm\imath\hat{q}$ of order two from the energy spread function, and then there is a pole at $\imath s - \hat{C}_{3D}$ from the oscillating term. The location of that pole affects the integration procedure, particularly if $\text{Re}(s) = 0$ so that the pole is on the real line (see figure 4.2).

By carefully accounting for these contour integral issues, the value for $\hat{D}$ for a Lorentzian distribution is given by [8]

$$\hat{D} = \imath \left(s + \hat{q} + \imath\hat{C}_{3D} \right)^{-2} \tag{4.5}$$

48
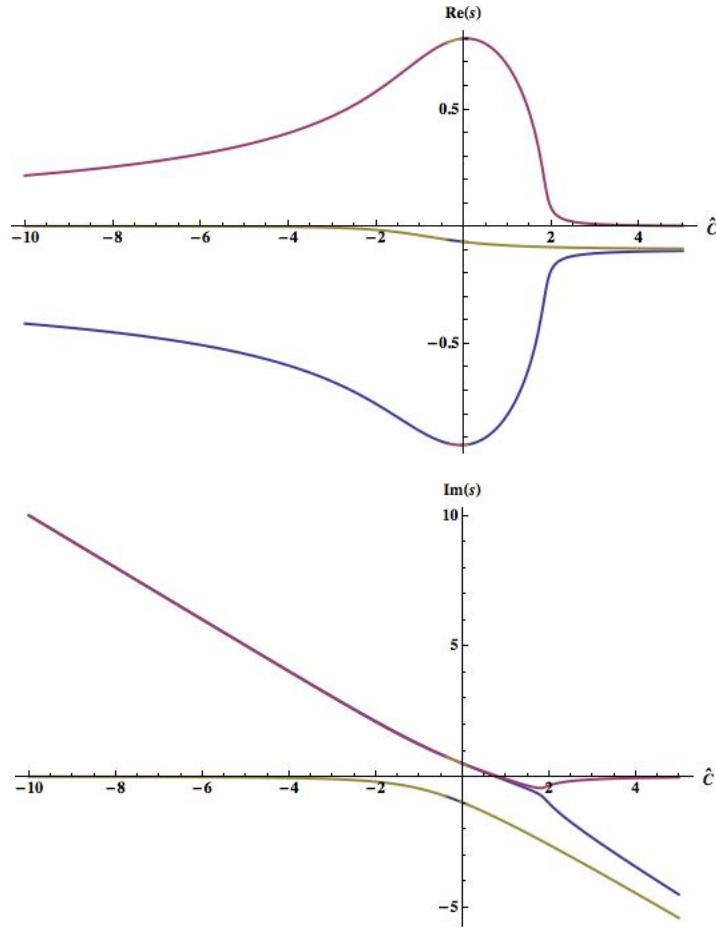
Figure 4.3: Gain curves for a $\kappa - 1$ distribution.

To illustrate the thermal effects on the roots of the dispersion relation, the real and imaginary parts of s for $\hat{q} = .1$ and $\hat{\Lambda}_p^2 = 0$ are presented in figure 4.3. In this figure, we show the three roots to the dispersion relation for the case when $\text{Re}(s) > 0$, as there are in fact three different dispersion relations depending upon the location of the $s + \imath(\hat{C} + \hat{P})$ pole relative to the closed contours.

49

Gaussian Distribution

The Lorentzian distribution is utilized as an approximation to the Gaussian energy distribution function

$$\hat{F} = \frac{1}{\sqrt{2\pi\hat{\Lambda}_T^2}} \exp\left[-\frac{\hat{P}^2}{2\hat{\Lambda}_T^2}\right] \tag{4.6}$$

As the contour integration method utilized for the Lorentzian beam is of no use in evaluating the Gaussian, I will omit the details of the calculation[1] and simply state the result as

$$\hat{D} = \imath \int_0^\infty \xi \exp\left\{-\frac{\hat{\Lambda}_T^2 \xi^2}{2} - \left(s + \imath\hat{C}_{3D}\right)\xi\right\} d\xi \quad \text{for Re } s > 0 \tag{4.7a}$$

$$\hat{D} = \imath \int_0^\infty \xi \exp\left\{-\frac{\hat{\Lambda}_T^2 \xi^2}{2} - \left(s + \imath\hat{C}_{3D}\right)\xi\right\} d\xi$$

$$-\imath\frac{\sqrt{2\pi}}{\hat{\Lambda}_T^3}(s + \imath\hat{C}_{3D})\exp\left\{\frac{\left(s + \imath\hat{C}_{3D}\right)^2}{2\hat{\Lambda}_T^2}\right\} \quad \text{for Re } s < 0 \tag{4.7b}$$

It is worth noting that a major restriction on the Gaussian distribution is that its solutions are not well-behaved for the inverse Laplace transform. Asymptotic solutions can be obtained, but there is no complete solution available for a Gaussian distribution. This is due to the nature of $\hat{D}$, which diverges as $\exp\left(s^2\right)$ along the imaginary s-axis, so that the Laplace transform is not well-behaved at $\pm\imath\infty$.

To get around this restriction, one method is to manipulate the contours to remove the offending poles at infinity and pick off the largest growing root.

---

[1]Details can be found in Chapter 2 of [8].

This root, for large $\hat{z}$, will dominate over the other roots with smaller real part. However this method is not satisfactory for applications to CeC, and so I present an alternative approach to building a Gaussian.

4.1 $\kappa - N$ Distributions

The exact analytical solutions for the electron screening in the pick-up [9] and analytical solutions in the kicker [15] are for the case of a $\kappa - 2$ distribution. The general form of the κ distribution is given by

$$f(x) \propto \frac{1}{(x^2 + q^2)^\kappa}$$

For the purposes of this dissertation, I only consider the case of κ as a positive integer, and the general $\kappa - N$ distribution function I utilize is given by

$$f_N(P) = \frac{\Gamma(N)}{\sqrt{2\pi N \sigma^2}\Gamma(N - 1/2)} \frac{1}{\left(1 + \hat{P}^2/(2\sigma^2 N)\right)^N} \qquad (4.8)$$

The choice for changing q as a function of N is made so that in the $N \to \infty$ limit, this distribution becomes the Gaussian distribution, and σ is fixed by the measurement of the RMS energy spread by assuming the true distribution is Gaussian.

The $\kappa - N$ distribution has poles of order N at $\pm i\sigma\sqrt{2N}$ which allows the identical contour integration method utilized for the Lorentzian to be carried out for arbitrary N [16] [14].

4.2 Dispersion Relation for $\kappa - N$

In the one-dimensional theory of small signal high-gain free-electron lasers, the growth of individual modes is determined by the roots of the dispersion relation

$$s - \frac{\hat{D}}{1 - \imath \hat{\Lambda}_p^2 \hat{D}} = 0 \qquad (4.9)$$

where

$$\hat{D} = \int d\hat{P} \, \frac{d\hat{F}}{d\hat{P}} \frac{1}{s + \imath(\hat{C} + \hat{P})} \qquad (4.10)$$

$\hat{F}$ is the normalized energy spread, and $\hat{\Lambda}_p^2$ is the space charge parameter, as defined in [8]. The space charge term is not expected to affect the physical results of this paper, and is therefore dropped from this point for the sake of simplicity.

For a lorentzian energy distribution, this equation may be evaluated exactly to give the familiar cubic equation for the dispersion relation. However, when this is applied to a gaussian energy distribution, closing the contours in the upper- or lower-half plane is not possible, as a gaussian diverges anywhere off the real axis as $R \to \infty$ in the complex plane. Because of this, only an asymptotic expression for the largest growing root can be obtained. This does not allow a study of the number and nature of the growing roots, which would be useful for studying short FELs.

Motivated by the existence of analytical solutions of other problems for applications in CeC [1] that consider dynamics in the pick-up [9] and kicker [15], we considered the case of a $\kappa - 2$ distribution to calculate the dispersion relation for a one-dimensional FEL. Realizing that the key to evaluating these

particular integrals is the existence of a pole in the upper- and lower-half plane, while vanishing along any closed contour, we were able to obtain a general formula for the dispersion relation of a high-gain FEL for any $\kappa - N$ distribution.

4.2.1 Evaluating $\hat{D}$ for $f_N(P)$

We define

$$\hat{D}_N = \imath \int d\hat{P} \; \frac{1}{\left(s + \imath(\hat{C} + \hat{P})\right)^2} f_N(\hat{P}) \tag{4.11}$$

which is equivalent to $\hat{D}$ for the Nth kappa distribution, and we have introduced normalized variables for direct comparison to [8]. For $\text{Re}(s) > 0$, the pole structure is given by fig. (4.2).

It is possible to close the contour in a half-plane in which only the imaginary axis pole is inside the contour for the growing or decaying roots, but for the oscillating root there is a half-contribution from the contour passing around a pole on the real axis. The imaginary axis contribution is given by

$$\phi_{\text{Im}} = -\frac{2\imath\pi}{(N-1)!} \frac{d^{N-1}}{d\hat{P}^{N-1}} \left[\left(s + \imath(\hat{C} + \hat{P})\right)^{-2} \left(1 - \imath\hat{P}/q_N\right)^{-N} (-\imath q_N)^N \right]_{\hat{P} = -\imath q_N} \tag{4.12}$$

which gives the resulting $\hat{D}_N$ in terms of the single pole

$$\hat{D}_N = \imath \frac{\Gamma[N]}{q_N \Gamma[N - 1/2]} \phi_{\text{Im}} \tag{4.13}$$

It can be shown that taking M derivatives of a product of two functions

behaves as a binomial expansion:

$$\frac{d^M}{dx^M}(f(x)g(x)) = \sum_{m=0}^{M} \binom{M}{m-1} f^{(m)}(x)g^{(M-m)}(x) \qquad (4.14)$$

This allows ϕ_{Im} to be solved as an expansion in the derivatives of the two components. The resulting series solution for $\hat{D}_N$ is given by

$$\hat{D}_N = \imath \frac{\Gamma[N]}{q_N \Gamma[N-1/2]} \times \frac{2\pi}{(N-1)!} \frac{1}{2^{2N-1}} \times$$

$$\sum_{m=0}^{N-1} \binom{N-1}{m} \left\{ \frac{2^m m!}{(s+q_N+\imath\hat{C})^{2+m}} q_N^{N-1-m} \frac{(2N-1-m)!}{(N-1)!} \right\} \qquad (4.15)$$

Solution of the dispersion equation (4.9) can then be obtained by whatever means are best.

4.2.2 The Roots for $\kappa - 2$

For the case of a $\kappa - 2$ distribution, which is valuable for the analytical work on CeC, I take $q_N = q_2 = q$ and obtain

$$\hat{D}_2^+ = \imath \frac{s+\imath\hat{C}+3q}{(s+q+\imath\hat{C})^3} \qquad (4.16)$$

This yields a fourth order equation in the dispersion relation, with the added condition that all roots must satisfy $\mathrm{Re}(s) > 0$ to obtain the growing roots. An analytical formula exists for the quartic, obtained by Ferarri's method, however the results are analytically complicated, and we present here only plots of the results. Supposing that $\sigma = .1$ for the definition of the q_N, this implies that

$q_2 = .2$, while the result for the Lorentzian distribution has $q_1 = .141$. We also consider the case of $\kappa - 5$ to illustrate how quickly this series begins to converge. For comparison purposes, I present on the same plot the results for both in figure $(4.4)^2$.
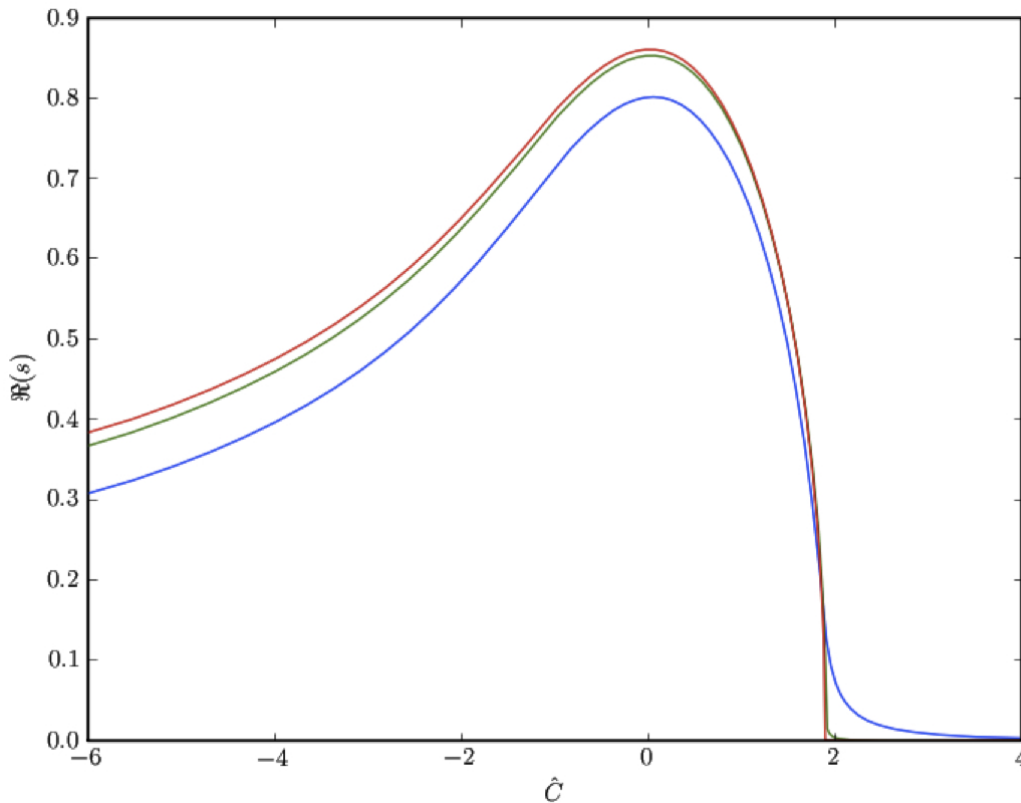
Figure 4.4: Growth rates for the $\kappa - 1$ distribution (blue), $\kappa - 2$ distribution (green) and $\kappa - 5$ distribution (red).

There is a small difference between the $\kappa - 1$ and $\kappa - 2$ distribution, most noticeable at zero detuning.

4.3 Number of Roots

Determining the number of growing modes is interesting when studying these problems as there is the outstanding question of how many modes there are that participate in the FEL amplification process. It turns out that there is always only one amplifying mode solution for any FEL dispersion relation, given sufficient criterion. To prove this, I develop a treatment for the FEL dispersion relation similar to the treatment for linear circuits first developed by Herbert Nyquist [17].

The idea behind this treatment is the application of the Argument Principle from complex analysis to the Laplace transform response function of a linear system, the dispersion relation in this case. The Argument Principle is precisely stated in the Appendix, but for here it is sufficient to state that, given a closed contour C in the complex plane and a function $f(z)$, then the difference in the number of poles and zeros is given by

$$Z - P = \frac{1}{2\pi} \oint_C d \, \arg(f(z)) \tag{4.17}$$

This allows anyone to calculate the difference between the number of zeros and the number of poles inside a given contour.

For the linear response function we consider, the number of amplifying modes is related to the number of modes where $\text{Re}(s) > 0$, so the choice of contour should obviously be a half-circle that encloses the right half-plane, as in figure (4.5).

This contour can be parameterized into two curves, one an arc given by
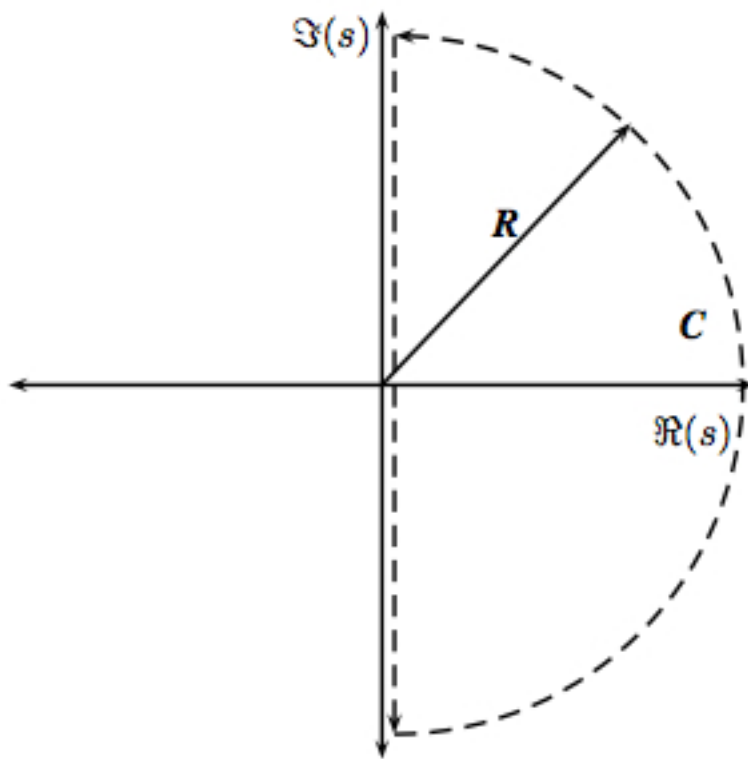
Figure 4.5: Contour for evaluating total number of roots

$s = Re^{it}$ for $t \in (\pi/2, -\pi/2]$ in the limit of $R \to \infty$, and the vertical line parameterized by $s = \epsilon + it$ for $\epsilon > 0$ and $t \in (-\infty, \infty)$. This parameterization should be able to include every zero and pole in the right half-plane of the complex s-plane for the dispersion relation.

First, I must account for the poles in the right half-plane. Such poles could only originate from poles in $\hat{D}(s)$, and therefore I consider the evaluation of the integral in equation (4.10) in very general terms.

From the requirement of causality, the integration must be taken first on the assumption that $\text{Re}(s) > 0$. If $\hat{F}(\hat{P})$ is some rational function with no poles on the real line, then it is reasonable to take the contour integration in evaluating this integral over the lower half of the complex $\hat{P}$-plane. Once this choice is made, the pole due to $(s + i(\hat{C} + \hat{P}))^{-1}$ must remain above the contour of integration. Because of the form of the integral, a pole in the lower half-plane in $\hat{P}$ will manifest as a pole in the left half-plane in the complex s-plane. This is clearly the case for any rational functional form of $\hat{F}(\hat{P})$. Transcendental functions – such as a gaussian distribution – can be written as the limit of a sequence of rational approximations (such as the definition of e^x or successive Padé approximants). So long as the poles do not flip signs or cross the real axis for any single term in the sequence, it is reasonable to assume that the poles will remain in the left half-plane of the complex s-plane. Therefore, $P = 0$ for this particular contour, and the number of zeros with $\text{Re}(s) > 0$ is equal to the winding number of the function around the above contour.

The change in the argument must be calculated in the counter-clockwise direction. For the arc, as $R \to \infty$, the contribution due to $\hat{D}(s)$ vanishes as
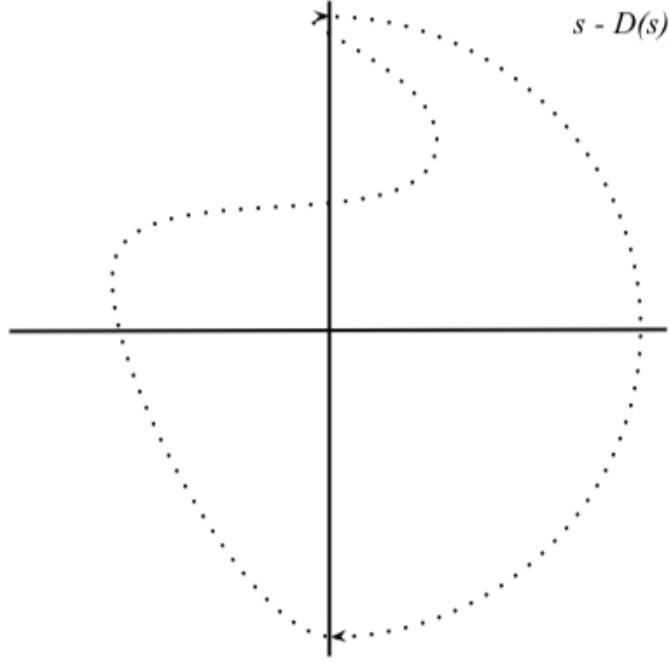
Figure 4.6: Contour for evaluating total number of roots. This corresponds to one growing root.

$\mathcal{O}(R^{-2})$, and so there is a change in the argument of $+\pi$ along that part of the contour. Thus, this contour of the mapping $s \mapsto w(s)$ is the identity mapping.

The real part of the dispersion relation along this contour is given by

$$\mathrm{Re}\left(\int d\hat{P} \frac{d\hat{F}}{d\hat{P}} \frac{1}{i(t + \hat{C} + \hat{P})}\right) \tag{4.18}$$

From the identity due to Landau that

$$[\cdots]\frac{1}{x}dx = \mathcal{P}\left([\cdots]\frac{1}{x}\right)dx + i\pi[\cdots]\delta(x)dx \tag{4.19}$$

59

where $\mathcal{P}$ denotes the Cauchy Principle Value, this may be expressed as

$$\mathrm{Re}\left(\int d\hat{P}\frac{d\hat{F}}{d\hat{P}}\frac{1}{\imath(t+\hat{C}+\hat{P})}\right)=$$
$$\mathrm{Re}\left(\mathcal{P}\int d\hat{P}\frac{d\hat{F}}{d\hat{P}}\frac{1}{\imath(t+\hat{C}+\hat{P})}+\pi\hat{F}'(\hat{P}=-t-\hat{C})\right) \tag{4.20}$$

Since the Cauchy Principle Value integral is pure imaginary, that component drops out and we are left with the criterion that

$$\hat{F}'(\hat{P}=-t-\hat{C})=0 \tag{4.21}$$

To deal with the winding of the vertical part of the contour, it is necessary to count how many times the vertical line wraps around the origin before the contour closes on itself. This is best done by counting where and when the mapping along the contour crosses the real axis, i.e. when $\mathrm{Re}(w(s=\imath t))=0$. To keep book, two bits of information are necessary: where the curve is crossing the the imaginary axis and whether it's crossing from left to right or from right to left. Where the crossing occurs is straightforward to calculate. If it is crossing from left to right or right to left can be determined by the derivative of $\hat{F}'$ at that point, which is the second derivative of $\hat{F}$. Thus, crossing from left to right corresponds to a negative derivative of $\hat{F}'$ and a local maximum of the distribution, while a crossing from right to left is a local minimum. If the zeros are ordered in descending value of t^* as $\{t_1, t_2, \ldots, t_n\}$ they must alternate crossing left-right or right-left. From understanding whether each one crosses left-right or right-left, and where, a schematic of the diagram can be developed and the winding number calculated fairly directly.

For a single bell-shaped curve the structure of $\hat{F}(\hat{P})$ with local maximum at $\hat{P} = 0$, $t = -\hat{C}$ is the only zero for finite values of t. This means that there is at most one growing mode under the definition used in this dissertation, and that for some $\hat{C}^*$ it crosses the zero line so that frequencies at detuning less than $\hat{C}^*$ are exponentially damped.

Plugging in $t = -\hat{C}$ into the dispersion integral, it is clear that the sign change occurs at

$$\hat{C}^* = \text{Im}\left[\int d\hat{P} \, \frac{d\hat{F}}{d\hat{P}} \frac{1}{\imath \hat{P}} \right] \tag{4.22}$$

As an example, for a properly normalized gaussian $\hat{F}$ with spread parameter $\hat{\Lambda}_T^2$, $\hat{C}^* = -\hat{\Lambda}_T^{-2}$. More generally it is clear from dimensional considerations that if $\hat{F}$ has only one energy spread parameter, $\hat{q}$, that $\hat{C}^* \sim \hat{q}^{-2}$. This result is similar to the result obtained for a free Coulomb plasma by Penrose [18] as a criterion for the onset of instability.

4.4 Conclusion

A closed form series for the dispersion integral for the FEL process was presented by evaluating the contour integration of a $\kappa - N$ distribution. Using this result I presented numerical evaluation of the roots to illustrate the rapid convergence in N, which converges to a Gaussian distribution for large N. This rapid convergence of the sequence of dispersion relations leading to the Gaussian distribution is encouraging.

Furthermore, I presented results that are topological in the sense that they depend only on the bell-shaped curve of the energy distribution function.

These results are totally general, and provide basic criterion for certain analytical properties of the dispersion relation for any choice of energy distribution that is reasonable for an electron bunch. In particular, the most compelling result is that there is always one and only one mode which is amplified by the FEL process, and all other modes are transients which decay exponentially or, at most, oscillate and become exponentially small by comparison to the primary growing mode.

I furthermore presented a set of criterion that includes the importance of space charge, and at least at what order of magnitude the space charge parameter may be expected to begin affecting the FEL amplification process.

Part II

Coherent Electron Cooling

5

Coherent Electron Cooling

The three-dimensional theory of FELs presented in this dissertation was developed to calculate the cooling decrement for Coherent Electron Cooling (CeC). CeC is intended to provide order of magnitude luminosity increases for the proposed eRHIC/MEeRHIC upgrade by rapidly increasing the phase space density of the hadron bunches. In this section, I discuss briefly the primary mechanisms of beam heating in RHIC, the method of stochastic cooling that has been implemented at RHIC, and a comparison with the method of coherent

electron cooling.

5.1 Beam Heating

The primary source of beam heating at RHIC is intra-beam scattering (IBS). In a free Coulomb gas, scattering exchanges phase space volume until an equilibrium is reached. For bunched beams in a storage ring there is dispersion, which couples the energy deviation from the design energy to the transverse motion. Under these circumstances, it is possible for a Coulomb scattering event to heat particles in all directions, so that a final equilibrium state is never reached.

Consider a physical picture of IBS due to Piwinski [19], illustrated in figure 5.1. In the lab frame, the bunch has very little transverse and longitudinal momentum spread, and is strongly biased in the longitudinal direction. However, in the rest frame, the bunch is essentially a Maxwellian gas interacting through the Coulomb interaction. Suppose two particles with perfectly transverse momentum in the rest frame scatter so that the resulting momentum all goes into the longitudinal direction. Because of the existence of dispersion in the lattice, the transverse betatron oscillation is given by

$$x_\beta = x - D\frac{\Delta p}{p} \tag{5.1}$$

where D is the dispersion of the lattice and p is the longitudinal design momentum. The longitudinal emittance increases after a longitudinal momentum spread is added. Because of dispersion, the transverse emittance can also
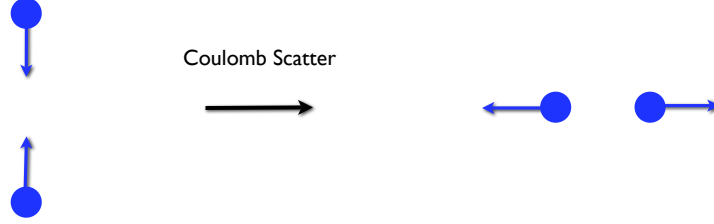
Figure 5.1: Piwinski picture of intrabeam scattering

change, and the total change at the point x on the lattice is given by

$$\Delta(\epsilon_{x,1} + \epsilon_{x,2}) = 2\frac{\pi}{\beta_x}\frac{p_x^2}{p}\left\{(D\gamma)^2 - \beta_x^2\right\}$$ (5.2)

The transverse coupling means that this particular interaction can increase the transverse emittance if $(D\gamma/\beta_x)^2 > 1$. In this way, the collision can heat both the transverse and longitudinal directions simultaneously!

IBS was described by Bjorken and Mtingwa [20] with the relevant equations for emittance exchange between the transverse and longitudinal directions due to Coulomb scattering, yielding a total growth rate in terms of lattice parameters and the properties of the individual bunches. A simplified treatment [21] gives the longitudinal growth rate as

$$\tau_\parallel^{-1} = \frac{r_i^2 c N_i \Lambda}{8\beta^3\gamma^3\epsilon_x^{3/2}\langle\beta_\perp^{1/2}\rangle\sqrt{\pi/2}\sigma_s\sigma_p^2}$$ (5.3)

and the transverse growth rate is given by

$$\tau_\perp^{-1} = \frac{\sigma_p^2}{\epsilon_x} \left\langle \frac{D_x^2 + (D_x'\beta_x + \alpha_x D_x)^2}{\beta_x} \right\rangle \tag{5.4}$$

where the brackets average over the ring lattice, D is the dispersion function, σ is the spread parameter (assuming a gaussian distribution), N_i is the number of particles in the bunch, r_i is the classical radius of these particles, and Λ is a Coulomb logarithm.

5.2 Stochastic Cooling

Stochastic cooling was proposed by van der Mier [22] as a method of using the discrete nature of bunched beams to provide cooling. For this work he was awarded the Nobel Prize in Physics in 1984 along with Carlo Rubio for stochastic cooling's contribution to the discovery of the W and Z bosons at the UA1 experiment at the Super Proton Synchrotron.

The process of stochastic cooling can be broken into three parts: the pick-up, amplifier and kicker. The pick-up samples the bunches with a bandwidth W and a decay time for the impulse response of a single particle given by $\tau \approx 1/2W$ [23]. Within this bandwidth N_s particles are detected by the pick-up. In the kicker, the target particle and all the other particles within the bandwidth are given an energy update

$$\bar{\epsilon}_k = \epsilon_k - \frac{g}{N_s} \sum_{m=1}^{N_s} \epsilon_m \tag{5.5}$$

where g is the gain. If the particle energies are uncorrelated, taking an ensem-

ble average gives the new energy variance as

$$\langle \bar{\epsilon}^2 \rangle - \langle \epsilon^2 \rangle = (-2g + g^2)\langle \epsilon^2 \rangle / N_s \tag{5.6}$$

which gives an optimal cooling at $g = 1$. To lowest order this gives an average cooling time of

$$\frac{1}{\tau} = \frac{2W}{N} \tag{5.7}$$

where N is the total number of particles in the system, given by $N_s = N/(2WT)$.

Because stochastic cooling as implemented at RHIC is bandwidth limited to between 5 and 8 GHz, which limits the cooling of intense bunches. Developed a system with substantially higher bandwidth is necessary for cooling more intense bunches, and in this sense Coherent Electron Cooling is an almost infinite bandwidth (on the order of 10 THz) stochastic cooling system.

5.3   Coherent Electron Cooling

Schematically, Coherent Electron Cooling (CeC) is identical to stochastic cooling. The primary difference is in the physical mechanisms of the pick-up, amplifier and kicker (see figure (5.2)).

The pick-up is the modulator, and uses dynamical Debye screening as described in [9] to create a charge perturbation with a longitudinal Debye radius on the order of the resonant wavelength of the free-electron laser, $r_D \sim \lambda_r$. In the FEL, this signal is amplified into a wave packet with wavelength λ_r, meanwhile the hadrons are given an energy-dependent delay using a disper-
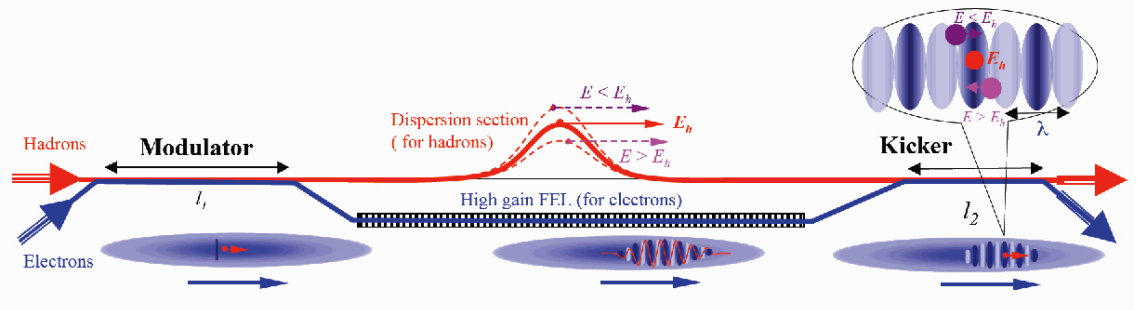
Figure 5.2: Schematic of Coherent Electron Cooling [1]

sive section (chicane). The hadron is then recombined with its now frequency-modulated and amplified signal, receiving an energy dependent kick of the form

$$\dot{\epsilon} = -\xi_0 \sin(k_r D_\ell \epsilon) \tag{5.8}$$

where ξ_0 is the cooling parameter, k_r is the resonant wavenumber of the FEL, and D_ℓ is the strength of the dispersive section [1]. The cooling decrement parameter is bounded above by

$$\xi_0 \leq 2\frac{G_0 \sigma_{z,e}}{\sigma_\delta \sigma_{z,h}} \frac{Z^2}{A} \frac{r_p}{\epsilon_{\perp n}} \tag{5.9}$$

where G_0 is the FEL gain, σ is the RMS spread, and $\epsilon_{\perp n}$ is the normalized transverse emittance of the electron bunch.

Incorporating the synchrotron oscillations, which are fast compared to the cooling time, gives an equation of motion for the envelope function of the synchrotron oscillations as

$$a' = -\xi_0 J_1(a) \tag{5.10}$$

where $J_1(x)$ is the first order Bessel function. For sufficiently large energy deviation, this leads to an antidamping instability, but for practical applications very few of the particles in the hadron bunches are located in this regime.

This model does not account for the inhomogeneities of the electron bunches, which are generally shorter than the hadron bunches and have to paint the hadron bunches. In the following chapter, I present a generalization of the above cooling equations to account for these two effects.

6

Dynamics of Coherent Electron Cooling

with Synchrotron Oscillations

In this chapter I present work for the dynamics of realistic Coherent Electron Cooling of bunched hadron beams. Beginning from a model set of non-hamiltonian equations for the energy and RF phase equations, and considering scaling laws for FEL parameters, I provide a detailed derivation of results presented in [24]. These equations are analytically intractable, but do provide

some insight into the dynamics of CeC, and can be quickly numerically solved to generate a phase space diagram for CeC neglecting effects of intra-beam scattering.

6.1   Electron Beam Inhomogeneities

The theoretical picture of high gain FEL operation in the previous chapter assumed an infinitely long, homogeneous electron beam passing through the undulator. In this case, infinitely long means that the beam is very long relative to the slippage length of the FEL. Over this relatively short length scale, the FEL model presented above represents a good picture of how an initial phase space perturbation amplifies into a frequency-modulated pulse. However, for the purposes of CeC it is necessary to consider how this particular amplification may change along the length of the electron bunches.

From the one-dimensional theory of FELs in [5], [6], etc., and knowing that $g_0 \propto f_1$, the FEL perturbation, this gives a scaling law that

$$g(\theta) = \tilde{g}\rho \ e^{z/L_G} \tag{6.1}$$

where L_G is the FEL gain length and $\rho = (k_w L_G)^{-1}$ is the Pierce parameter. What is relevant here is that $L_G \propto n_0(\theta)^{-1/3}$. This allows me to rewrite the cooling rate parameter in the original CeC equation as

$$g(\theta) = g_0 \ n(\theta)^{1/3} \ e^{n(\theta)^{1/3}\hat{z}_0} \tag{6.2}$$

where $n(\theta)$ is the distribution of electrons in the bunch as a function of the

hadron bunch RF phase, normalized so that the peak is at $\theta = 0$ and $n(0) = 1$, so that $\hat{z}_0$ is the normalized undulator length for the peak current and g_0 is the cooling decrement for this peak current.

The most analytically convenient distribution to consider at this point is one with bounded support, taking

$$n(\theta) = (1 - \theta^2/\theta_0^2)^3 \; \Theta(1 - |\theta/\theta_0|) \tag{6.3}$$

where Θ is the Heaviside step function and θ_0 is the electron bunch length. To convert θ_0 to the RMS bunch length, I assume that the bunch is effectively zero density at three sigma, so $\theta_0 = 3\,\sigma_e$.

6.2   CeC Dynamic Equations: Short Electron Bunches

In a practical application of Coherent Electron Cooling planned as a proof of principle, the parameters for the electron bunches leave them shorter than the hadron bunches by approximately a factor of two, and in practice this requires scanning the entire hadron beam many times, and considering a cooling rate that is dependent upon the RF phase of the particle being cooled.

In the original CeC paper [1] the dynamic equation for bunched hadron beams was given by

$$\epsilon' \approx -g_0 \sin(k D_\ell \epsilon) \tag{6.4}$$

where $\epsilon = (E_0 - E)/E_0$ is the normalized energy deviation. Synchrotron

oscillations were added phenomenologically in the form of $\epsilon = a \sin(\Omega_s n + \psi_s)$ and an equation for a was derived assuming g_0 to be a constant. In practice, g_0 will be a complicated function of the RF phase θ and this interaction must be considered in greater detail.

I begin with the non-hamiltonian system of equations for small synchrotron oscillations and inhomogeneous cooling, given by

$$\dot{\epsilon} = g(\theta) \sin(kD_\ell \epsilon) + V_0 \theta \tag{6.5a}$$

$$\dot{\theta} = -\eta \epsilon \tag{6.5b}$$

where V_0 is the RF cavity energy and η is the phase slip factor.

To model the scanning over the bunches, I assume that $\theta \mapsto \theta + p(\omega t)$, where $p(\omega t)$ is a periodic function that sweeps over some length of the hadron bunches. From these considerations, the CeC equations for a bunched beam are given by

$$\dot{\epsilon} = g_0 \left(1 - \frac{\phi^2}{\theta_0^2}\right) \Theta(1 - |\phi|/\theta_0) \exp\left\{ \left(1 - \frac{\phi^2}{\theta_0^2}\right) \hat{z}_0 \right\} \sin(kD_\ell \epsilon + \frac{1}{\sqrt{3}} \frac{\phi^2}{\theta_0^2} \hat{z}_0) + V_0 \theta \tag{6.6a}$$

$$\dot{\theta} = -\eta \epsilon \tag{6.6b}$$

where the $\phi = \theta + f(\omega t)$.

Assuming that $\hat{z}_0 \gg 1$ the step function can be dropped as any nonzero contribution too far from $\phi = \theta_0$ will be exponentially small. The above equations can then be rewritten in normalized form by taking $\hat{\epsilon} = kD_\ell \epsilon$ and pulling the constant exponential under g_0 to give the cooling decrement ξ_0,

and the equations

$$\dot{\epsilon} = \hat{\xi}_0 \left(1 - \frac{\phi^2}{\theta_0^2}\right) \Theta(1 - |\phi|/\theta_0) \exp\left\{\left(-\frac{\phi^2}{\theta_0^2}\right)\hat{z}_0\right\} \sin\left(\hat{\epsilon} + \frac{1}{\sqrt{3}}\frac{\phi^2}{\theta_0^2}\hat{z}_0\right) + \hat{V}_0\theta$$

(6.7a)

$$\dot{\theta} = -\hat{\eta}\epsilon$$

(6.7b)

There are three relevant time scales – the synchrotron oscillation frequency $\Omega_s = \sqrt{\eta V_0}$, the painting frequency of the beam ω, and the CeC cooling rate $\tau_{CeC}^{-1} = \xi_0$. In order, $\Omega_s \gg \omega \gg \tau_{CeC}^{-1}$ and this hierarchy allows a number of approximations. The first is to remove the fast-oscillating synchrotron oscillations using the two-time formalism (see, for example, [25]). Under this formalism, define $\tau = \Omega_s t$ and $T = \hat{\xi}_0 \tau$, so that

$$\frac{d}{dt} = \Omega_s^{-1}\partial_\tau + \Omega_s^{-1}\xi_0\partial_T$$

(6.8)

and then match perturbation theory order by order in $\hat{\xi}_0$, i.e. $\hat{\epsilon} = \hat{\epsilon}^0 + \hat{\xi}_0\hat{\epsilon}^1 + \ldots$ and the same for θ. To lowest order this given solutions for the energy deviation and synchrotron phase as

$$\hat{\epsilon}^0(\tau, T) = A(T)\sin(\tau + \Psi(T))$$

(6.9a)

$$\theta^0(\tau, T) = A(T)\hat{\eta}\cos(\tau + \Psi(T))$$

(6.9b)

To next order in $\hat{\xi}_0$ the energy deviation satisfies the equation

$$\partial_\tau^2\hat{\epsilon}^1 + \hat{\epsilon}^1 = -\partial_\tau\left(2\partial_T\hat{\epsilon}^0 + f(\theta^0, \hat{\epsilon}^0)\right)$$

(6.10)

75

where

$$f(\theta, \hat{\epsilon}) = \left(1 - \frac{\phi^2}{\theta_0^2}\right) \exp\left\{\left(-\frac{\phi^2}{\theta_0^2}\right)\hat{z}_0\right\} \sin\left(\hat{\epsilon} + \frac{1}{\sqrt{3}}\frac{\phi^2}{\theta_0^2}\hat{z}_0\right) \qquad (6.11)$$

The first order perturbation is not expected to have secular terms causing growth, so the first order harmonic of the right hand side has to vanish. That is to say, if $\psi = \tau + \Psi(T)$ then

$$\int_{-\pi}^{\pi} d\psi \; \sin\psi \; \left(2\partial_T\hat{\epsilon}^0 + f(\theta, \hat{\epsilon})\right) = 0 \qquad (6.12a)$$

$$\int_{-\pi}^{\pi} d\psi \; \cos\psi \; \left(2\partial_T\hat{\epsilon}^0 + f(\theta, \hat{\epsilon})\right) = 0 \qquad (6.12b)$$

The first equation yields a differential equation in T that involves just $A(T)$, since the $\Psi(T)$ dependence is integrated out. The second equation gives a differential equation for $A\partial_T\Psi$ that is a pure function of T once the first differential equation in $A(T)$ is solved. Therefore, I focus entirely on the results of the first equation for the evolution of the envelope function. By a symmetry argument which removes the part of f even in ψ, the differential equation for $A(T)$ can be reduced to

$$\frac{dA}{dT} = -\int_{-\pi}^{\pi} d\psi \; \sin\psi \; \left(1 - \frac{\phi^2}{\theta_0^2}\right) \exp\left\{-\frac{\phi^2}{\theta_0^2}\hat{z}_0\right\} \sin(\hat{\epsilon}^0) \cos\left(\frac{\phi^2}{\sqrt{3}\theta_0^2}\hat{z}_0\right) \qquad (6.13)$$

where $\phi = \theta^0 + p(\omega t)$.

Dealing term by term with the Bessel function expansions:

$$\sin(\hat{\epsilon}^0) = J_0(A) + 2\sum_{n=1}^{\infty} J_n(A)\sin(n\psi) \qquad (6.14)$$

76

$$\cos\left(\frac{\phi^2}{\sqrt{3}\theta_0^2}\hat{z}_0\right) = \cos\left[\frac{A^2\hat{\eta}^2\cos^2\psi}{\sqrt{3}\theta_0^2}\hat{z}_0 + \frac{2A\hat{\eta}p\cos\psi}{\sqrt{3}\theta_0^2}\hat{z}_0\right]\cos\left(\frac{p^2\hat{z}_0}{\sqrt{3}\theta_0^2}\right)$$
$$- \sin\left[\frac{A^2\hat{\eta}^2\cos^2\psi}{\sqrt{3}\theta_0^2}\hat{z}_0 + \frac{2A\hat{\eta}p\cos\psi}{\sqrt{3}\theta_0^2}\hat{z}_0\right]\sin\left(\frac{p^2\hat{z}_0}{\sqrt{3}\theta_0^2}\right) \tag{6.15}$$

For this term, I exploit the identities that

$$\exp(\imath z\cos\alpha) = \sum_{n=-\infty}^{\infty}\imath^n J_n(z)e^{\imath n\alpha} \tag{6.16}$$

and drop fast-oscillating terms in ψ to give that

$$\cos\left(\frac{\phi^2}{\sqrt{3}\theta_0^2}\hat{z}_0\right) \approx \left\{\cos\left(\frac{A^2\hat{\eta}^2\hat{z}_0}{2\sqrt{3}\theta_0^2}\right)\cos\left(\frac{p^2\hat{z}_0}{\sqrt{3}\theta_0^2}\right) - \sin\left(\frac{A^2\hat{\eta}^2\hat{z}_0}{2\sqrt{3}\theta_0^2}\right)\sin\left(\frac{p^2\hat{z}_0}{\sqrt{3}\theta_0^2}\right)\right\} \times$$
$$J_0\left(\frac{A^2\hat{\eta}^2\hat{z}_0}{2\sqrt{3}\theta_0^2}\right)J_0\left(\frac{2A\hat{\eta}p\hat{z}_0}{\sqrt{3}\theta_0^2}\right) \tag{6.17}$$

Dropping all the higher harmonic terms that are higher harmonic than the term proportional to $J_1(A)\sin\psi$ and all other terms orthogonal to $\sin\psi$ under the integration leaves

$$f(\theta^0,\hat{\epsilon}^0) \approx \exp\left(-\frac{A^2\hat{\eta}^2}{2\theta_0^2}\hat{z}_0\right)J_0\left(\frac{A^2\hat{\eta}^2\hat{z}_0}{2\theta_0^2}\right)\frac{p^2}{\theta_0^2}e^{-p^2\hat{z}_0/\theta_0^2} \times$$
$$\left[\cos\left(\frac{A^2\hat{\eta}^2\hat{z}_0}{2\sqrt{3}\theta_0^2}\right)\cos\left(\frac{p^2\hat{z}_0}{\sqrt{3}\theta_0^2}\right) - \sin\left(\frac{A^2\hat{\eta}^2\hat{z}_0}{2\sqrt{3}\theta_0^2}\right)\sin\left(\frac{p^2\hat{z}_0}{\sqrt{3}\theta_0^2}\right)\right] \times \tag{6.18}$$
$$J_0\left(\frac{A^2\hat{\eta}^2\hat{z}_0}{2\sqrt{3}\theta_0^2}\right)J_0\left(\frac{2A\hat{\eta}p\hat{z}_0}{\sqrt{3}\theta_0^2}\right)J_1(A)\sin\psi$$

Taking the $\sin\psi$ integration gives the envelope equation as

$$
\frac{dA}{dT} = -J_1(A)\exp\left\{-\frac{A^2\hat{\eta}^2}{2\theta_0^2}\hat{z}_0\right\} J_0\left(\frac{A^2\hat{\eta}^2}{2\theta_0^2}\hat{z}_0\right) J_0\left(\frac{A^2\hat{\eta}^2}{2\sqrt{3}\theta_0^2}\hat{z}_0\right) \times
$$
$$
\left[\cos\left(\frac{A^2\hat{\eta}^2\hat{z}_0}{2\sqrt{3}\theta_0^2}\right)\cos\left(\frac{p^2\hat{z}_0}{\sqrt{3}\theta_0^2}\right) - \sin\left(\frac{A^2\hat{\eta}^2\hat{z}_0}{2\sqrt{3}\theta_0^2}\right)\sin\left(\frac{p^2\hat{z}_0}{\sqrt{3}\theta_0^2}\right)\right] \times \quad (6.19)
$$
$$
\left(1 - p^2/\theta_0^2\right) J_0\left(\frac{2A\hat{\eta}p}{\sqrt{3}\theta_0^2}\hat{z}_0\right)\exp\left\{-p^2\hat{z}_0/\theta_0^2\right\}
$$

The first line of the equation comes purely from the finite size of the electron bunch. $J_1(A)$ is the bare cooling function, while the Gaussian envelope and first J_0 come from gain loss due to lower electron bunch density at the edges of the bunches. The second J_0 on that line comes from the phase shift due to the changing electron density in the bunch. The second two lines come entirely from the painting scheme, and it is simple enough to see that if $p = 0$ then the equation works purely by cooling the center of the hadron bunches with strong attenuation at the edges.

The painting time being much less than the cooling time, it is sensible to take some averaging over the painting. If a single cycle of the painting takes place over $T \in (-T_{paint}, T_{paint})$ then I define the average painting as

$$
\left\langle\frac{dA}{dT}\right\rangle_{paint} = -J_1(A)\exp\left\{-\frac{A^2\hat{\eta}^2}{2\theta_0^2}\hat{z}_0\right\} J_0\left(\frac{A^2\hat{\eta}^2}{2\theta_0^2}\hat{z}_0\right) J_0\left(\frac{A^2\hat{\eta}^2}{2\sqrt{3}\theta_0^2}\hat{z}_0\right) \times
$$
$$
\frac{1}{2T_{paint}}\int_{-T_{paint}}^{T_{paint}} dt \left[\cos\left(\frac{A^2\hat{\eta}^2\hat{z}_0}{2\sqrt{3}\theta_0^2}\right)\cos\left(\frac{p^2\hat{z}_0}{\sqrt{3}\theta_0^2}\right) - \sin\left(\frac{A^2\hat{\eta}^2\hat{z}_0}{2\sqrt{3}\theta_0^2}\right)\sin\left(\frac{p^2\hat{z}_0}{\sqrt{3}\theta_0^2}\right)\right] \times
$$
$$
\left(1 - p^2/\theta_0^2\right) J_0\left(\frac{2A\hat{\eta}p}{\sqrt{3}\theta_0^2}\hat{z}_0\right)\exp\left\{-p^2\hat{z}_0/\theta_0^2\right\}
$$

$$
(6.20)
$$

where, recall, $p = p(t/T_{paint})$ and $\omega = 2\pi/T_{paint}$ as used earlier.

6.3   Painting Schemes

In this section I consider some numerical forms for the cooling equation above, considering first an even painting, linear in time, and then a painting that lingers near the edges. First, I assume that $A \ll 1$ so that $J_1(A) \approx A$ and the equation can be reduced to an almost dimensionless form. Defining

$$\hat{A} = \frac{A\hat{\eta}\sqrt{\hat{z}_0}}{\sqrt{2}\theta_0} \tag{6.21}$$

and

$$\hat{p} = \frac{p\sqrt{\hat{z}_0}}{\theta_0} \tag{6.22}$$

and normalizing $\tau = t/T_{paint}$ gives

$$\frac{1}{\hat{A}}\frac{d\hat{A}}{dT} = -\frac{1}{2}\exp\left\{-\hat{A}^2\right\} J_0\left(\hat{A}^2\right) J_0\left(\hat{A}^2/\sqrt{3}\right) \times$$

$$\frac{1}{2}\int_{-1}^{1} d\tau \ \left[\cos\left(\hat{A}^2/\sqrt{3}\right)\cos\left(\hat{p}^2/\sqrt{3}\right) - \sin\left(\hat{A}^2/\sqrt{3}\right)\sin\left(\hat{p}^2/\sqrt{3}\right)\right] \times \quad (6.23)$$

$$\left(1 - \hat{p}^2/\hat{z}_0\right) J_0\left(\hat{A}\hat{p}/\sqrt{3}\right)\exp\left\{-\hat{p}^2\right\}$$

This equation leaves a handful of free parameters: the amplitude and functional form of the painting scheme (which is now assumed to be periodic with period 2), and the length of the FEL amplifier.

It is worth noting that, in practice, the normalized $\hat{A}$ is of the same order of magnitude as A (for the parameters used in [24] the constant of proportionality is 2.77). Therefore the objective should be to create as flat a cooling rate as possible for $A \lesssim 1$.
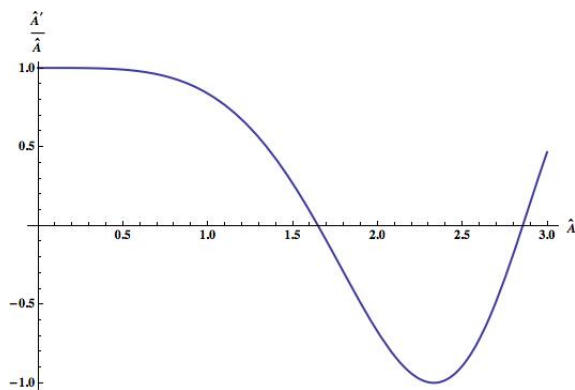
Figure 6.1: Cooling rates for zero painting

6.3.1 Zero Painting

I begin by considering the absence of painting, which gives a baseline on which to measure the performance of the various painting schemes.

In this case, the dimensionless cooling rate is given by figure 6.1. This gives anti-damping beyond $\hat{A} \gtrsim 1.5$, which for the given parameters limits the damping to inside $A \lesssim .54$. This is the edge of the linear approximation for $J_1(x) \approx x/2$, so no painting would have the effect of covering the entire linear bare cooling regime.

However, it is desirable to keep a more constant cooling rate over the entire duration to prevent creating local inflection points in the density of hadrons, which can lead to various instabilities.

6.3.2 Linear Painting

Consider a linear painting in which $\hat{p} = a\tau$. The cooling functions, on the right hand side of the cooling equation (6.23), are given below for a number of parameters. There is a competition between making the amplitude of the
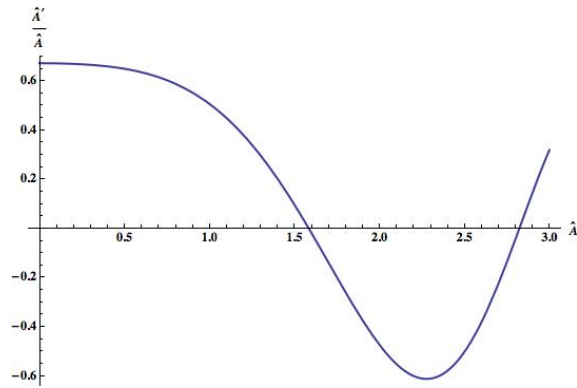
Figure 6.2: Cooling rates for linear painting out to $\hat{A} = 1$
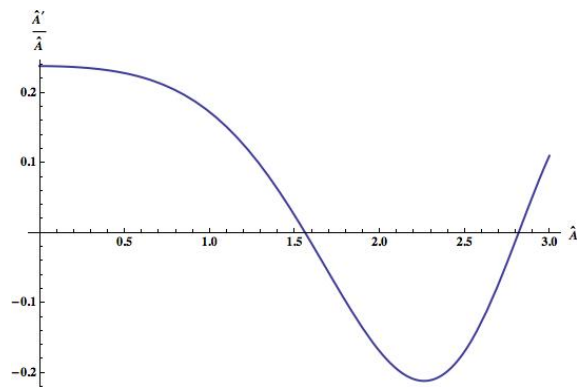
Figure 6.3: Cooling rates for linear painting out to $\hat{A} = 3$

cooling too large, which reduces the overall cooling rate, and making it too small, which may not adequately cool the hadron bunch.

Clearly painting out does not extend the flat initial cooling rate out very far, and indeed painting too far out strongly suppresses the cooling rate on the tails.
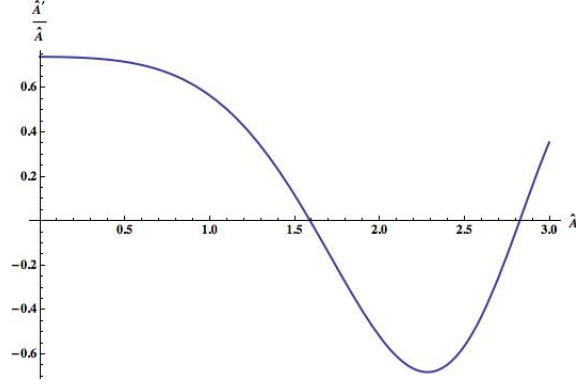
Figure 6.4: Cooling rates for edge painting with $\tau_{rise} = 1$ and $p_0 = 1$
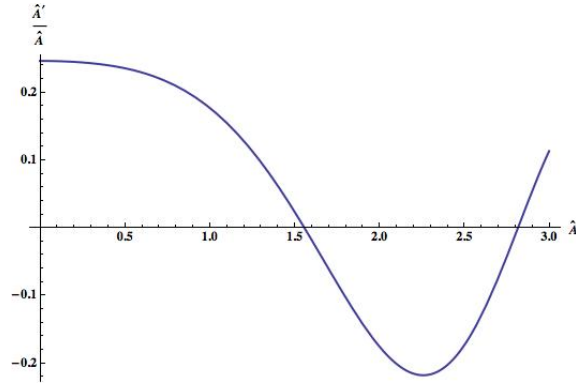
Figure 6.5: Cooling rates for edge painting with $\tau_{rise} = 1$ and $p_0 = 3$

6.3.3 Edge-Emphasized Painting

To enhance cooling at the edges, I next consider a painting scheme of the form

$$\hat{p}(\tau) = p_0 \tanh\left(\tau/\tau_{rise}\right) \tag{6.24}$$

This paint scheme has the advantage of spending more time at the edges than at the center of the hadron bunches, which cools the tails more than the core.

By considering the various paint schemes, it would appear to be quite
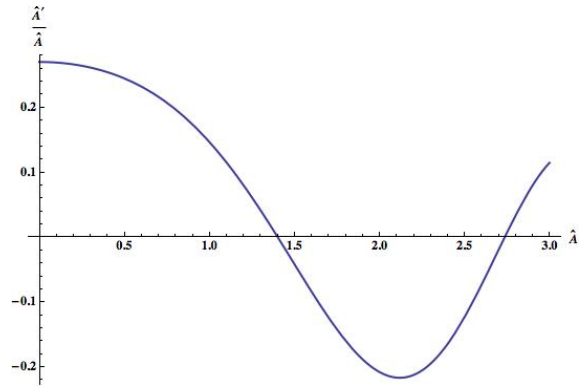
Figure 6.6: Cooling rates for edge painting with $\tau_{rise} = 0.1$ and $p_0 = 1$
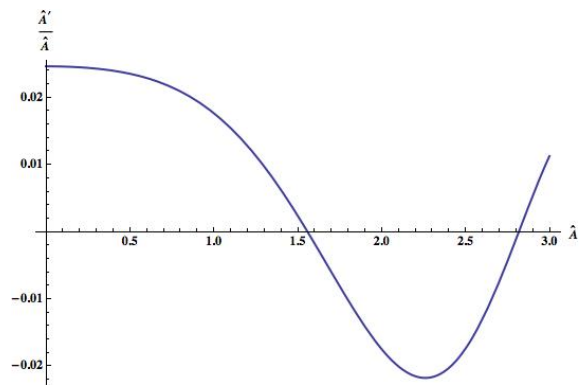
Figure 6.7: Cooling rates for edge painting with $\tau_{rise} = .1$ and $p_0 = 3$

83

difficult to extend the location of the crossing over to cool greater amplitudes. The difficulty comes from the gaussian damping due to the paint scheme.

From these considerations, it is clear that the specifics of the paint scheme are more or less irrelevant. What is more important is to consider optimizing the ratio $\hat{\eta}\sqrt{\hat{z}_0}/\theta_0$ to be as small as possible. This expands the range going from $\hat{A}$ to A to include a larger range of synchrotron amplitudes. A reduction in $\hat{z}_0$ reduces the cooling decrement ξ_0 so that the best way to handle cooling would be to use long electron bunches or have a small phase slip parameter.

6.4   CeC Kinetic Equation

I will conclude this chapter with a discussion of the Coherent Electron Cooling kinetic equation, to include the effects of intra-beam scattering diffusion and the CeC cooling rate.

Begin by defining the cooling equation as

$$Q(A) = -\hat{A}\frac{1}{2}\exp\left\{-\hat{A}^2\right\}J_0\left(\hat{A}^2\right)J_0\left(\hat{A}^2/\sqrt{3}\right)\times$$
$$\frac{1}{2}\int_{-1}^{1}d\tau\ \left[\cos\left(\hat{A}^2/\sqrt{3}\right)\cos\left(\hat{p}^2/\sqrt{3}\right)-\sin\left(\hat{A}^2/\sqrt{3}\right)\sin\left(\hat{p}^2/\sqrt{3}\right)\right]\times\quad(6.25)$$
$$\left(1-\hat{p}^2/\hat{z}_0\right)J_0\left(\hat{A}\hat{p}/\sqrt{3}\right)\exp\left\{-\hat{p}^2\right\}$$

This particular equation for A, which is proportional to the action of a simple harmonic oscillator in the RF cavity, is non-hamiltonian. To treat this, I consider the treatment derived in [26] with no two-particle correlations, thereby making this treatment simpler. This derivation follows closely the one presented there.

For a system with N particles and a phase space of variables $\{(q_i, p_i)\}_{0 \leq i \leq N}$ an ensemble distribution $D(\{(q_i, p_i)\})$ normalized to unity requires that the total number of particles is conserved. Mathematically, this is expressed as

$$\frac{\partial D}{\partial t} + \boldsymbol{\nabla} \cdot (\boldsymbol{u}D) = 0 \tag{6.26}$$

where $\boldsymbol{u} = (\{(\dot{q}_i, \dot{p}_i)\})$ and $\boldsymbol{\nabla} = \partial_{vecq} + \partial_{\boldsymbol{p}}$. I will later add a phenomenological intra-beam scattering diffusion term For the small amplitude RF oscillations and the cooling, using the normalized coordinates, the equations of motion are given by

$$\dot{A} = \xi_0 Q(A) \tag{6.27a}$$

$$\dot{\psi} = 1 \tag{6.27b}$$

where $\dot{x}$ is a time derivative with respect to $\tau = \Omega_s t$. From this set of equations the statement of particle number conservation becomes

$$\frac{\partial D}{\partial t} + \sum_{i=1}^{N} \partial_{A_i}(\xi_0 Q(A_i)D) + \partial_{\psi_i} D = 0 \tag{6.28}$$

Because we are only interested in a single-body distribution function, and the distribution of amplitudes, I integrate over the measure

$$\int dA_2 \ldots dA_N d\psi_1 \ldots d\psi_N$$

to obtain as an expression for the single-particle amplitude distribution func-

tion $F(A, t)$ in the absence of intra-beam scattering as

$$\partial_t F(A, t) + \partial_A \left(\xi_0 Q(A) F(A, t) \right) = 0 \qquad (6.29)$$

This equation predicts the particles will pile up at the origin. However, intra-beam scattering introduces a synchrotron oscillation averaged diffusion term on the right-hand side as a source of phase space expansion, so that the kinetic equation for Coherent Electron Cooling is given by

$$\partial_t F(A, t) + \partial_A \left(\xi_0 Q(A) F(A, t) \right) = \partial_A \left(D_{IBS}(A) \partial_A F(A, t) \right) \qquad (6.30)$$

This gives as a solution for the equilibrium distribution the familiar result

$$F(A) = F_0 \exp \left\{ \int dA \xi_0 \frac{Q(A)}{D_{IBS}(A)} \right\} \qquad (6.31)$$

6.5 Conclusion

In this chapter I have presented a calculation for the cooling equations of Coherent Electron Cooling. By considering the scaling laws of the relevant FEL parameters, I developed an approximate expression for the cooling decrement of synchrotron oscillations in terms of their envelope function. From this equation, I was able to write down a kinetic equation for Coherent Electron Cooling that considers synchrotron oscillations, the painting scheme, and the CeC cooling, as well as intra-beam scattering or other diffusive effects.

7

Conclusion

Coherent electron cooling represents a huge potential in the field of cooling intense, relativistic beams. Its effectively infinite bandwidth and rapid cooling capabilities are of great interest for making order of magnitude improvements in the luminosities of intense hadron beam colliders, such as the proposed eRHIC upgrade. To develop a complete picture of the theory of coherent electron cooling, a three-dimensional model of free-electron lasers had to be developed, as well as an understanding of the cooling effects on the phase space

distribution of bunched beams.

It was the purpose of this dissertation to present a three-dimensional theory of free-electron lasers for applications to coherent electron cooling. This theory is compatible with its beam model to the work in [9] and in [15] in that it allows for consideration of an infinite electron beam. The model provides an analytical solution in Fourier-Laplace space, and can be solved in terms of an initial phase space perturbation.

In developing this three-dimensional FEL model for infinite beams, a finite beam model arose naturally from the derivation, and presented an opportunity to consider and characterize the nature of optical guiding. This model predicts the prevalence of a single eigenmode in propagation, and the extent to which that mode expands can be calculated directly.

Finally, a system of equations was presented for the dynamics of synchrotron oscillations for Coherent Electron Cooling which incorporates beam inhomogeneities in the electron bunch, synchrotron oscillations, and the painting scheme. The painting scheme was developed to maximize the rate of cooling of the RMS spread in the amplitude of synchrotron oscillations.

A

A Crash Course on Accelerator Physics

Throughout this dissertation I have used the language of accelerator physics. Most prevalent are the concepts of betatron oscillations, synchrotron oscillations, and emittance. In this appendix I will summarize each concept for the convenience of those uninitiated into the accelerator community. The conventions of this section are taken from a technical note by Sands [27].

A.1 Betatron Oscillations

Storage rings such as the Tevatron, the Relativistic Heavy Ion Collider and the Large Hadron Collider use the principle of strong focusing first proposed by Courant, Livingston and Snyder at Brookhaven National Lab [28]. Under the principle of strong focusing, a series of quadrupole magnets behave like hyperbolic lenses, defocusing charged particles in one transverse direction while focusing them in the other. With this analogy to ray tracing, by stringing together a series of focusing and defocusing lenses with proper focal lengths, a net focusing effect is created. The resulting oscillations of particles offset from the design orbit are called *betatron oscillations*.

Shifting to radial coordinates and carrying out a coordinate transformation to remove the design orbit, the betatron orbit is described by

$$x''_\beta = K_x(s)x_\beta \tag{A.1}$$

where

$$K_x(s) = -\left(\frac{ecB_0(s)}{\mathcal{E}_0}\right)^2 - \frac{ec}{\mathcal{E}_0}\left(\frac{\partial B_0}{\partial x}\right)_{0s} \tag{A.2}$$

with B_0 being the magnitude of the magnetic field along the design orbit parameterized by the longitudinal coordinate s. For a storage ring, clearly $K_x(s + L) = K_x(s)$ for some L, and this problem becomes similar to the problem of solving the Schrödinger equation in a periodic potential.

Because the equation for x_β is linear, a general superposition of sine and cosine like terms is possible, and in accelerator physics this are parameterized

by declaring that

$$x(s) = a\sqrt{\beta(s)}\cos(\phi(s) + \vartheta) \tag{A.3}$$

$\beta(s)$ is the much-ballyhooed *betatron function* and amounts to an envelope function. Because of the above differential equation, the phase advance is related to the betatron function by

$$\phi(s) = \int_0^s \frac{ds'}{\beta(s')} \tag{A.4}$$

so the betatron function is an effective wavelength of betatron oscillations. Defining $\zeta^2 = \beta$, the betatron function satisfies the nonlinear differential equation

$$\zeta'' = K(s)\zeta + \frac{1}{\zeta^3} \tag{A.5}$$

It's clear from this that the betatron function never becomes zero, and that the transverse size of any bunch is well-parameterized and understood in terms of the betatron function.

Because of this nonlinearity, it is convenient to define an average betatron number by

$$\oint \frac{ds}{\beta(s)} = \frac{L}{\beta_n} \tag{A.6}$$

where L is the periodicity of the storage ring. This gives an average betatron oscillation given by

$$x(s) \approx a\sqrt{\beta_n}\cos(s/\beta_n + \vartheta) \tag{A.7}$$

and defines the *betatron tune* ν as

$$\frac{L}{\beta_n} = 2\pi\nu \qquad\qquad (A.8)$$

For reasons of avoiding resonances, there are a variety of constraints on ν when designing a storage ring lattice. Further discussion along these lines is interesting, but beyond the scope of this dissertation.

A.2 Synchrotron Oscillations

In bunched beams stored in a synchrotron, clusters of particles are stored through the lattice of steering and focusing magnets, but they are accelerated by an RF cavity. A particle arriving at a time T in the phase of the RF cavity will receive an energy kick equal to

$$\bar{\epsilon} = \epsilon + V_0 \sin(\omega_{rf}T) \qquad\qquad (A.9)$$

The time of flight τ for a particle between successive turns is given by

$$\frac{\delta T}{T_0} = \alpha\frac{\bar{\epsilon}}{E_0} \qquad\qquad (A.10)$$

where E_0 is the design energy and α is an average of the magnetic field strength related to off-energy betatron oscillations. In practice, this leads to a set of equations given by

$$\frac{d\epsilon}{dt} = V_0 \sin(\omega_{rf}\tau + \phi_s) \qquad\qquad (A.11a)$$

$$\frac{d\tau}{dt} = -\alpha \frac{\epsilon}{E_0} \tag{A.11b}$$

where $T = T_0 + \tau$ and T_0 is the transit time for the synchronous particle. This is a pendulum type equation, and the resulting oscillations are referred to as *synchrotron oscillations.*

A.3 Emittance

Emittance is a measure of the beam quality, and measure the combined spread in a coordinate and its canonical conjugate. For a given variable y and its derivative y', the emittance of an ensemble of particles where $\langle y \rangle = 0$ and $\langle y' \rangle = 0$ is given by

$$\epsilon_{rms} = \sqrt{\langle y^2 \rangle \langle y'^2 \rangle - \langle yy' \rangle} \tag{A.12}$$

For relativistic particles this emittance is not conserved through acceleration, even if the beam quality remains fixed. This is because the canonical variable $p_y = py' = mc\beta\gamma y'$ varies with γ. Therefore the *normalized emittance* is defined by $\epsilon_n = \beta\gamma\epsilon$ and is fixed throughout acceleration.

The emittance gives a rough estimate of the transverse size of the beam. For a betatron function $\beta(s)$ and a gaussian beam profile, the transverse size is given by

$$\sigma_y = \sqrt{\beta(s)\epsilon/\pi} \tag{A.13}$$

This is relevant for the figure of merit for colliders, the *luminosity*. The lumi-

nosity of a given collider is given by

$$\mathcal{L} = 2fN_1N_s \int dx dz ds d(\beta ct)\rho_1(x, z, s + \beta ct)\rho_2(x, z, s - \beta ct) \qquad \text{(A.14)}$$

for a given distribution function of the bunches, where N is the number of particles in the bunch and f is the frequency of collisions. The emittance is directly related to these probability distribution functions ρ_i, and coherent electron cooling seeks to make the distributions as narrow as possible to maximize the above integral.

B

Gauge Transformation and Vanishing ϕ

The Maxwell equations have a gauge freedom in defining the four-vector potential that does not affect the result for the electric or magnetic fields. In particular, since

$$\boldsymbol{E} = -\nabla\phi - \frac{1}{c}\frac{\partial}{\partial t}\boldsymbol{A} \qquad \text{(B.1a)}$$

$$\boldsymbol{B} = \nabla \times \boldsymbol{A} \qquad \text{(B.1b)}$$

the following mapping can be made, with the choice of gauge Λ. Taking $\boldsymbol{A} \mapsto \boldsymbol{A} + \nabla\Lambda$ and $\phi \mapsto \phi + c^{-1}\partial_t\Lambda$ or, in relativistic four-vector notation

$$A^\mu \mapsto A^\mu + \partial^\mu\Lambda \tag{B.2}$$

maintains the physical form of the magnetic and electric fields.

From this gauge freedom it is clear that a single component of A^μ can be forced to vanish, and in the case being considered it is the scalar potential that is best removed. To achieve this, define

$$\Lambda = \int^t dt'\phi(t', \boldsymbol{r}_\perp, z) \tag{B.3}$$

This removes the scalar potential, which greatly simplifies the hamiltonian given by equation 3.7. Because this expression is independent of the choice of space-coordinates, this choice of gauge will also work to have the scalar potential vanish for any number of spatial dimensions. Therefore, we may assume throughout this dissertation that the scalar potential is zero, for both the one-dimensional and three-dimensional models.

C
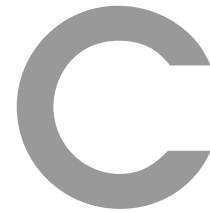
Canonical Transformations

The Hamilton equations of motion can be derived from a least-action principle on the action integral given by

$$\Phi[p, q] = \int p^\mu dx_\mu = \int \boldsymbol{p} \cdot d\boldsymbol{x} - \mathcal{H} dt \qquad \text{(C.1)}$$

For the case where t is the independent variable, the familiar Hamilton equations arise. If, for example, z is taken as the independent variable, the new

action integral is minimized with respect to z trajectories in terms of $d\boldsymbol{x}_\perp/dz$ and dt/dz instead of the more commonly used velocities. The resulting equations of motion are given by

$$\frac{d\boldsymbol{p}_\perp}{dz} = \frac{\partial p_z}{\partial \boldsymbol{x}_\perp} \tag{C.2a}$$

$$\frac{d\boldsymbol{x}_\perp}{dz} = -\frac{\partial p_z}{\partial \boldsymbol{p}_\perp} \tag{C.2b}$$

$$\frac{d\mathcal{H}}{dz} = -\frac{\partial p_z}{\partial t} \tag{C.2c}$$

$$\frac{dt}{dz} = \frac{\partial p_z}{\partial \mathcal{H}} \tag{C.2d}$$

The equations of motion for any arbitrary set of coordinates may be obtained from the action integral C.1 with the appropriate substitutions. This formalism makes canonical transformations transparent, as they are simply the set of mappings $p^\mu(P^\mu, Q_\mu)$ and $q_\mu(P^\mu, Q_\mu)$ that maintains the form

$$\int p^\mu dq_\mu \mapsto \int P^\mu dQ_\mu \tag{C.3}$$

As a quick example of this, consider a situation in which it is convenient to define the coordinate $q_1 = x + y$. To create canonical coordinates, we have to have a set of variables that preserves the form of the action integrand. We therefore write that

$$p^x dx + p^y dy - \mathcal{H}dt = p^1(dx + dy) + p^2 dq_2 - \mathcal{H}dt \tag{C.4}$$

It is possible to then make $dq_2 = dy$, for example, and then require that $p^1 +$

$p^2 = p^y$ and $p^1 = p^x$. This requires that we define the canonical transformation to be

$$p^1 = p^x \tag{C.5a}$$

$$p^2 = p^y - p^x \tag{C.5b}$$

This removes the need to write down a generating function, as per the standard methods presented in texts such as [29].

It is also convenient for non-canonical transformations, as the resulting equations are still the correct equations of motion, even if they are no longer symplectic. An example of such a transformation would be to introduce the ponderomotive phase $\psi = k_w z + \omega(z/c - t)$ as a coordinate, but not making the requisite change in the canonical hamiltonian and momenta to maintain the canonical form. This case can be considered for FEL theory, but is not the formalism chosen for the approach of this dissertation. I mention it here purely for completeness, and because of the clarity of exposition that arises from considering hamiltonian mechanics in this light.

Noting that $d\psi = (k_w + \omega/c)dz - \omega dt$, the action integral can be rewritten as

$$\Phi = \int \left(p_z - (k_w + \omega/c)\frac{\mathcal{H}}{\omega} \right) dz - \frac{\mathcal{H}}{\omega} d\psi \tag{C.6}$$

If we wanted to make these equations canonical, we would write that $H = \mathcal{H}/\omega$ being canonically conjugate to ψ and $\mathcal{P} = p_z - (k_w + \omega/c)\mathcal{H}/\omega$ as canonically conjugate to z. This is a great example of how this action integral formalism can immediately lead to canonical coordinate transformations. However the point being illustrated here is maintaining non-canonical coordinates. In this

case, the least action principle gives the following equations to minimize the action

$$\frac{d}{dz}\frac{\partial \phi}{\partial \psi'} - \frac{\partial \phi}{\partial \psi} = 0 \tag{C.7a}$$

$$\frac{d}{dz}\frac{\partial \phi}{\partial \mathcal{H}'} - \frac{\partial \phi}{\partial \mathcal{H}} = 0 \tag{C.7b}$$

These are the familiar Euler-Lagrange equations. If these equations are followed to their proper end, they obtain identical equations of motion to those that would arise from introducing the $(H, \psi; \mathcal{P})$ canonical coordinate transformation.

As a final example of a situation in which canonically conjugate variables can be obtained from this method, I look at the simple harmonic oscillator, with a hamiltonian given by

$$\mathcal{H} = \frac{1}{2}p^2 + \frac{1}{2}\omega^2 q^2 \tag{C.8}$$

The action integral is given by

$$\int pdq - \mathcal{H}dt \tag{C.9}$$

Defining the momentum variable $a = p + \imath\omega q$, we seek a canonically conjugate variable. The hamiltonian is written as $\mathcal{H} = aa^*/2$, and it is sensible to use a^* as a second variable. The question is if this choice of coordinates is canonical, and what the resulting hamiltonian that generates the equations of motion is.

In this case, the action integral transforms to

$$\Phi[a, a^*] = \frac{1}{4\imath\omega}\left\{(a + a^*)da - (a + a^*)da^*\right\} - \frac{1}{2}aa^*dt \qquad \text{(C.10)}$$

This form is clearly not canonical, and therefore a and a^* are not canonically conjugate variables. However, minimizing the action integral leads to the equations of motion

$$\dot{a}^* = \imath\omega a \qquad \text{(C.11a)}$$

$$\dot{a} = -\imath\omega a^* \qquad \text{(C.11b)}$$

which may be confirmed to be the correct equations of motion by directly inserting the definitions of a and a^* into these equations. Therefore this method of least action obtains the correct equations of motion even for coordinate transformations which are not canonical.

By taking the hamilton equations of this hamiltonian we obtain the correct equations of motion. The purpose of this coordinate transformation was to illustrate the utility of such coordinate transformations in obtaining desired information from a coordinate system that is likely to greatly simplify matters.

D

Contour Integration, Laplace Transforms, and Other Mathematics of Interest

In this appendix I discuss in greater details some of the mathematics utilized in the paper that are probably familiar to the reader, but may require some brief review for all the details. Each section is meant to be complete,

but due to the overlap in many of the applications they are not self-contained. The inquiring reader is therefore advised to read this whole chapter, start to finish, and without complaint. More thorough discussions of what is outlined here may be found in Morse and Feshbach [30], Whittaker and Watson [31], Antimirov Kolyshkin and Vaillancourt [32] and in Tricomi [33].

D.1 Delta Function Properties, for Physicists that Already Know Them

The Dirac delta function is defined as a functional, so that if $f(x)$ is some function that is continuous at the point $x = a$ then

$$
\int_b^c f(x)\delta(x-a)dx = \begin{cases} 0 & a \notin [b,c] \\ f(a) & a \in [b,c] \end{cases}
\tag{D.1}
$$

Representations of the delta function include limits of all κ distributions in the infinitely narrow limit, as well as the infinitely narrow gaussian distribution. The key here is that the delta function be normalized to unity, zero everywhere but one point, and infinite at that point.

Of particular use to the work in this dissertation is the identity

$$
\delta(k) = \frac{1}{2\pi} \int_{-\infty}^{\infty} e^{\imath k x} \ dx
\tag{D.2}
$$

It should be clear that this integral is infinite if $k = 0$, but for $k \neq 0$ the question is why this integral is zero. The essential argument comes from

inserting a convergence factor $\exp(-\epsilon|x|)$ and then taking $\epsilon \to 0$. This answers the question quite nicely. A consequence of this Fourier integral identity is the frequently utilized identity

$$\int dr \; e^{-\imath q r} \int dk \; dk' \; e^{\imath(k+k')r} = \int dk \; dk' \delta\left(q - (k + k')\right) \quad \text{(D.3)}$$

which is applied in getting from equation 3.21 to equation 3.22. This result also appears frequently in Feynman diagrams as momentum-conserving integrals, and generally in any case where a convolution integral appears. More explicitly, consider an equation of the form

$$\int dr \; e^{-\imath q r} \int dk \; dk' \; e^{\imath(k+k')r} G(r) \quad \text{(D.4)}$$

This leaves application of the delta function integration gives

$$\int dk \; G(k - q) \quad \text{(D.5)}$$

This type of transformation appears in arriving at the kernel for the finite size beam theory of FELs presented in this dissertation.

D.2   Argument Principle

In Chapter 4, I used the Argument Principle to prove that under sufficient conditions the number of growing FEL modes is always one. The Argument Principle, properly stated, says

Let $f(z)$ be a meromorphic function in a simply connected domain

D bounded by the simple closed path C. Suppose that $f(z)$ has no zeros nor poles on C. Then the difference between the number of zeros, Z, and the number of poles, P, in D, counting orders, is given by the formula

$$Z - P = \frac{1}{2\pi} \mathrm{Var}_C \ \arg f(z) \qquad \text{(D.6)}$$

The proof of this depends on the existence of branch cuts, which I now provide:

Proof. Consider the contour integral

$$\frac{1}{2\pi i} \oint_C \frac{f'(z)}{f(z)} dz = \sum_k \mathrm{Res}_{z=\tilde{z}_k} \frac{f'(z)}{f(z)} + \sum_k \mathrm{Res}_{z=z_k} \frac{f'(z)}{f(z)} \qquad \text{(D.7)}$$

where $\tilde{z}_k$ is a zero of order n_k of $f(z)$ and z_k is a pole of order p_k of $f(z)$. The above summation becomes

$$\sum_k n_k - p_k = Z - P \qquad \text{(D.8)}$$

Now observe that $f'(z)/f(z) = d\ln(f(z))/dz$. The contour integral then becomes

$$Z - P = \frac{1}{2\pi i} \oint_C d\ln(f(z)) = \frac{1}{2\pi i} \oint_C d\ln(|f(z)|) + \frac{1}{2\pi} \oint_C d\arg f(z) \qquad \text{(D.9)}$$

The first integral vanishes, leaving only the second, thereby proving the Argument Principle. QED $\square$

The Argument Principle arises from the branch cuts of the natural logarithm in the complex plane, and is an essential way to calculate winding numbers, for example.

D.3 Laplace Transforms, and their Inverses

A function $f(t)$ has the Laplace transform $F(s)$ defined by the Laplace transform integral

$$F(s) = \int_0^\infty dt \ e^{-st} f(t) \tag{D.10}$$

It is clear from the definition that Laplace transformation is a linear operation, with all the identities that brings. Furthermore, it is invertible, with the inverse given by

$$\mathcal{L}^{-1}(F(s)) = \int_{-\imath\infty+\gamma_0}^{\imath\infty+\gamma_0} ds \ e^{st} F(s) = f(t) \tag{D.11}$$

where γ_0 is selected so that if $F(s)$ has poles at $s_1, s_2 \ldots s_n$, then $\gamma_0 > \sup\{\mathrm{Re}(s_i)\}$. It is interesting to note that Laplace transformation is a Wick rotation of Fourier transformation, under suitable conditions. If $F(s)$ has a few poles to the left of the vertical line on the complex plane that passes through the point on the real axis at $s = \gamma_0$, then those poles will determine the rate of exponential growth or decay, and oscillation frequency.

Among the useful properties of Laplace transformation is the *convolution property*, which states that

$$\mathcal{L}\left(\int^x f(x)h(x-y)dy\right) = \mathcal{L}(f(x))\mathcal{L}(h(x)) \tag{D.12}$$

This property will be exploited in a discussion of integral equations. Since Laplace transforms are very closely related to Fourier transforms, this identity can be seen as arising from equation D.3.

For the purposes of taking the Laplace transform of equation 3.26, it is necessary to evaluate integrals of the form

$$h(x) = \int_0^x dx'\ e^{\imath k(x'-x)} g(x') \tag{D.13}$$

where $g(x)$ will be various integrals or derivatives of the longitudinal current, for the purposes of this dissertation. Taking the Laplace transform of $h(x)$ gives

$$
\begin{aligned}
\int_0^\infty dx\ e^{-sx} h(x) &= \int_0^\infty dx\ e^{-sx} \int_0^x dx'\ e^{\imath k(x'-x)} g(x') \\
&= \int_0^\infty dx'\ e^{\imath k x'} g(x') \int_{x'}^\infty dx\ e^{-sx-\imath k x} \\
&= \int_0^\infty dx'\ e^{\imath k x'} g(x') \left(\frac{1}{s+\imath k} e^{-sx'-\imath k x'} \right) \\
&= \int_0^\infty dx'\ e^{-sx'} g(x') \frac{1}{s+\imath k} = G(s) \frac{1}{s+\imath k}
\end{aligned}
\tag{D.14}
$$

which is obtained by switching the order of integration (see figure D.1). This is also a special case of the convolution identity mentioned above.

This gives the Laplace transform for equation 3.26 directly, and it remains to add a table of various Laplace transform identities for easy pickings (see table D.1).
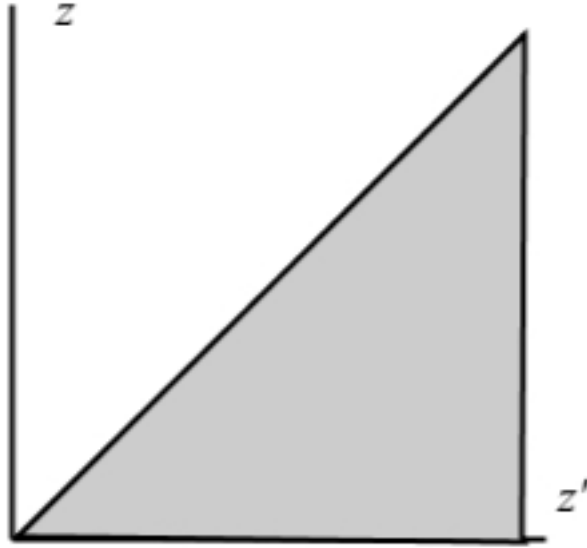
Figure D.1: The area of integration for the Laplace transform discussed in equation D.14.

Table D.1: Table of possibly relevant Laplace transforms.

Function	Laplace Transform
e^{kx}	$\frac{1}{s+k}$
$\tilde{j}_z$	J_z
$\int_0^z dz' \tilde{j}_z$	$\frac{1}{s} J_z$
$\frac{d}{dz} \tilde{j}_z$	$s J_z - \tilde{j}_z(z=0)$

Bibliography

[1] Vladimir N. Litvinenko and Yaroslav S. Derbenev. Coherent electron cooling. *Phys. Rev. Lett.*, 102(114801), 2009.

[2] John M. J. Madey. Stimulated emission of bremsstrahlung in a periodic magnetic field. *J. App. Phys.*, 42(5), 1971.

[3] D.A.G. Deacon, L.R. Alias, John M. J. Madey, G.J. Ramian, H.A. Schwettman, and T.I. Smith. First operation of a free-electron laser. *Phys. Rev. Lett.*, 38(16), 1977.

[4] A. M. Kondratenko and E. L. Saldin. Generation of coherent radiation by a relativistic electron beam in an undulator. *Part. Accelerators*, 10: 207–216, 1980.

[5] R. Bonifacio, C. Pellegrini, and L. Narducci. Collective instabilities and high-gain regime in free electron laser. *Opt. Commun.*, 50(6), 1984.

[6] E. L. Saldin, E. A. Schneidmiller, and M. V. Yurkov. Linear theory of the fel amplifier with planar undulator linear theory of the fel amplifier with planar undulator. *Nucl. Instrum. and Methods A*, 313(3), 1992.

[7] J. Murphy and C. Pellegrini. *Laser Handbook, Vol. 6*, chapter Introduction to the Physics of Free Electron Lasers. Elsevier, 1990.

[8] E. L. Saldin, E. A. Schneidmiller, and M. V. Yurkov. *The Physics of Free Electron Lasers*. Springer, 2000.

[9] G. Wang and M. Blaskiewicz. Dynamics of ion shielding in an anisotropic electron plasma. *Phys. Rev. E*, 76(026413), 2008.

[10] Stephen D. Webb, Gang Wang, and Vladimir N. Litvinenko. A 3-dimensional theory of free electron lasers. In *Proceedings of FEL10*, 2010.

[11] S.D. Webb, G. Wang, and V. N. Litvinenko. A three-dimensional model of small signal free-electron lasers. Submitted to PRST-AB, arXiv:1103.2676v1.

[12] A.A. Vlasov. The vibrational properties of an electron gas. *Sov. Phys. Usp.*, 93(3), 1968.

[13] S.P. Niles, J. Blau, and W. B. Colson. Hermite-gaussian decomposition of free electron laser optical fields. *Phys. Rev. ST-AB*, 2010.

[14] Stephen D. Webb and V. N. Litvinenko. Dispersion relations for small signal high-gain free-electron lasers. *Phys. Rev. E*, 2011.

[15] Gang Wang. The evolution of electron density modulation within a cec kicker. C-AD Lecture, August 2009.

[16] Stephen D. Webb and Vladimir N. Litvinenko. Dispersion relations for 1d high-gain fels. In *Proceedings of FEL10*, 2010.

[17] H. Nyquist. Regeneration theory. *Bell System Technical Journal*, 11, 1932.

[18] O. Penrose. Electrostatic instabilities of a uniform non-maxwellian plasma. *Phys. Fluids*, 3(2), 1960.

[19] A. Piwinski. Intra-beam scattering. In *Lecture Notes in Physics*, volume 296. Springer, 1988.

[20] J. D. Bjorken and S. K. Mtingwa. Intrabeam scattering. *Accelerator Physics*, 13:115–143, 1983.

[21] A. Fedotov. Comments on simplified treatment of intrabeam scattering. Technical Report C-A/AP/168, C-AD, Brookhaven National Laboratory, September 2004.

[22] D. Mohl, G. Petrucci, L. Thorndahl, and S. van der Meer. Physics and technique of stochastic cooling. *Phys. Rept.*, 58(2), 1980.

[23] M. Blaskiewicz, J.M. Brennan, and J. Severino. Operational stochastic cooling in the relativistic heavy-ion collider. *Phys. Rev. Lett.*, 2008.

[24] S.D. Webb and V.N. Litvinenko. Effects of e-beam parameters on coherent electron cooling. In *Proceedings of PAC11*, 2011.

[25] Steven H. Strogatz. *Nonlinear Dynamics and Chaos*. Addison Wesley, 1994.

[26] J. Bisgonano and C. Leeman. Stochastic cooling. Technical Report 14106, LBL, 1982.

[27] Matthew Sands. The physics of electron storage rings: An introduction. Technical Report 121, SLAC, 1979.

[28] E. D. Courant, M. Stanley Livingston, and H. S. Snyder. The strong-focusing synchrotron – a new high energy accelerator. *Phys. Rev.*, 88(5), 1952.

[29] H. Goldstein, C. Poole, and J. Safko. *Classical Mechanics*. Addison Wesley, third edition, 2002.

[30] Philip M. Morse and Herman Feshbach. *Methods of Theoretical Physics*. McGraw-Hill, 1953.

[31] E.T. Whittaker and G.N. Watson. *A Course of Modern Analysis*. Cambridge Mathematical Library. Cambridge University Press, 1927.

[32] M. Ya. Antimirov, A. A. Kolyshkin, and Remi Vaillancourt. *Complex Variables*. Academic Press, 1998.

[33] F.G. Tricomi. *Integral Equations*. Dover Publications, 1957.